Holistic research of diffusely reflected light in cellulosic materials

Satoru Tsuchikawa

Graduate School of Bioagricultural Sciences
Nagoya University, Japan

Wood has been used for thousands of years as
an environmentally friendly and renewable construction material

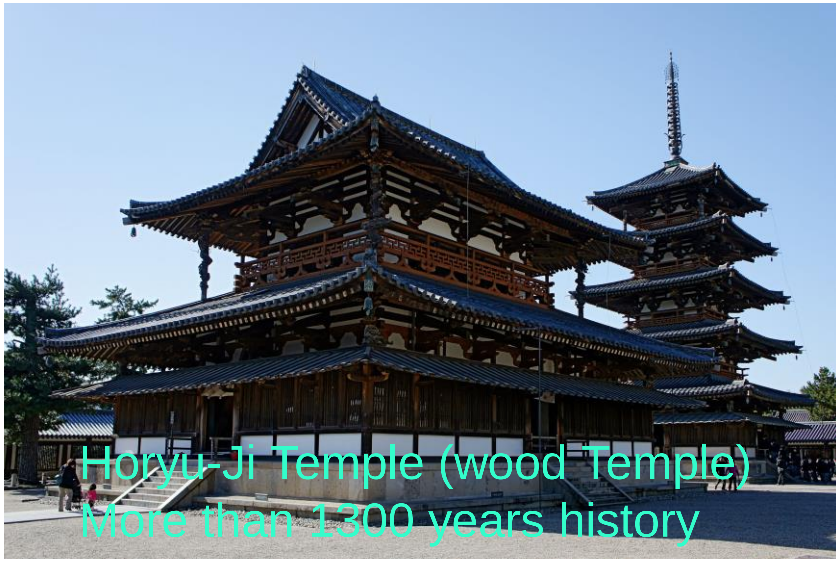

NIR Spectroscopy in Wood Science and Technology

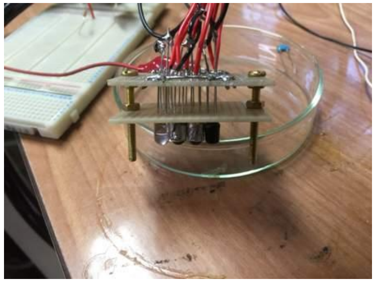

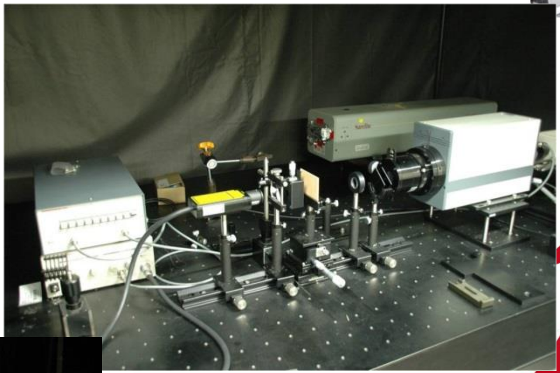

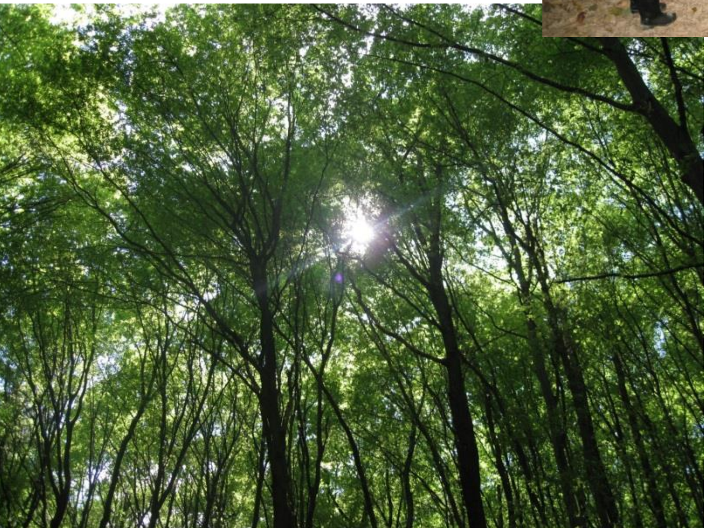

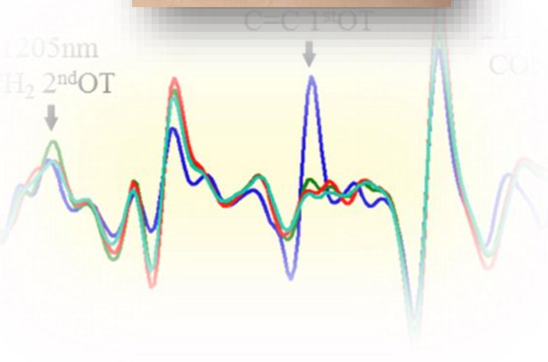

So far, over 500 NIR research aimed at the wood or paper science and industry have been published.
Most of them have been published in latter half of 1990s and 2000s.

1. WOOD CHEMISTRY AND PHYSICS
   - 1-1. Assignment of NIR Absorption Bands Related to Wood
   - 1-2. NIR Research for Chemical Composition of Wood (Lignin, Cellulose, Extractives)
   - 1-3. NIR Research for Physical Property of Wood (Moisture content, Grain angle and surface roughness, Density, Anatomical parameter, Mechanical property)

2. ENGINEERING WOOD

3. WOOD DEGRADATION AND MODIFICATION

4. PULP AND PAPER
   - Pulp and Paper Making System
   - Pulp Yield
   - Chemical Component of Pulp
   - Physical and Optical Research for Pulp and Paper

S. Tsuchikawa, *Applied Spectroscopy Reviews*, **42**: 43-71, 2007

S. Tsuchikawa and M. Schwanninger, *Applied Spectroscopy Reviews*, **48**: 560-587, 2013

Original and Second-Derivative NIR Spectra for Japanese Red Pine and Japanese Zelkova

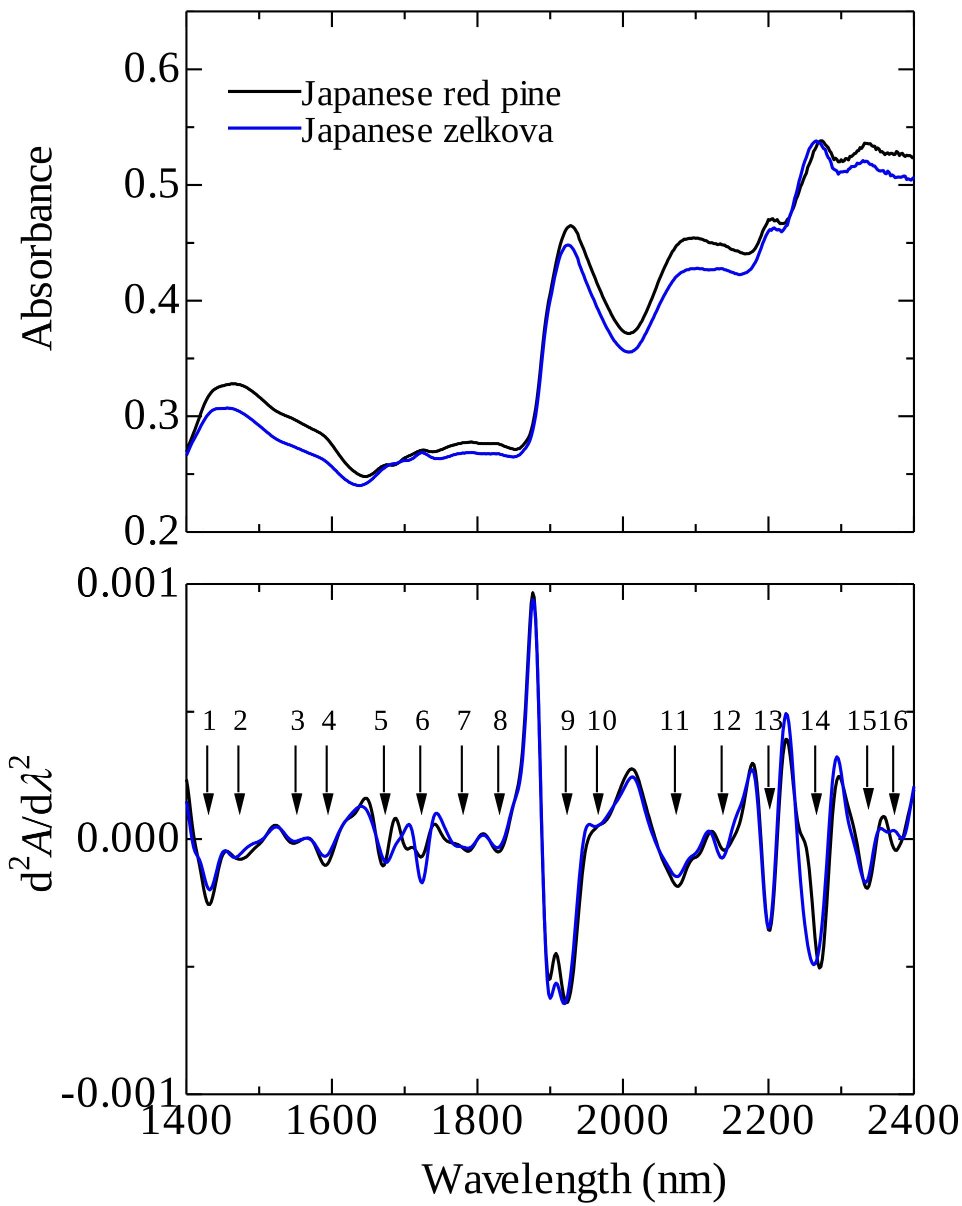

Assignment

1-4 : OH (Cellulose)
5 : CH (Lignin)
6 : CH (Hemicellulose)
7,8 : Cellulose
9,10 : OH (Water)
11,12 : OH (Cellulose)
13 : CHO
14 : ?
15 : CH (Cellulose)
16 : CH (Holocellulose)

Wood is a complex material
(Composed of cellulose, lignin, hemicellulose
and minor amounts of extractives)

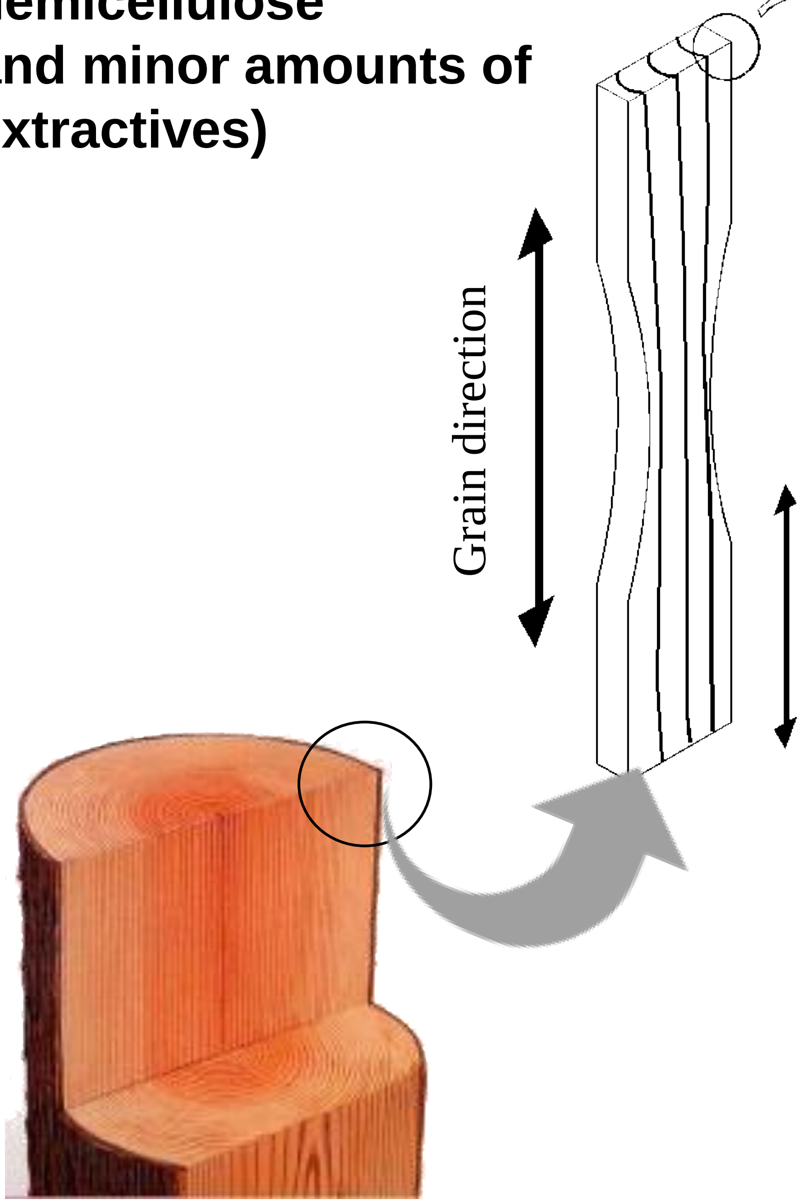

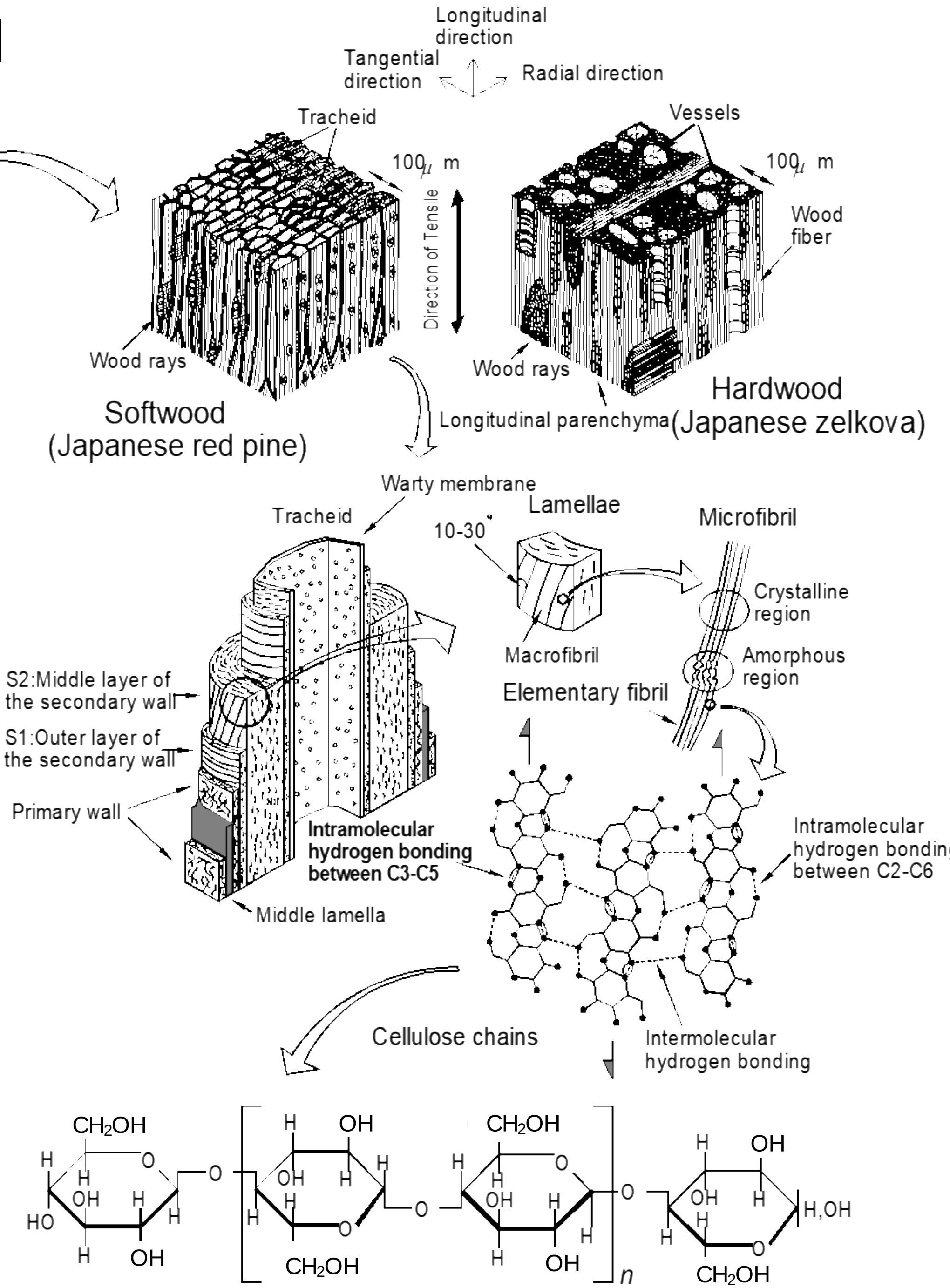

Topic I

Construction of Novel Wood Densitometer using NIR Laser System

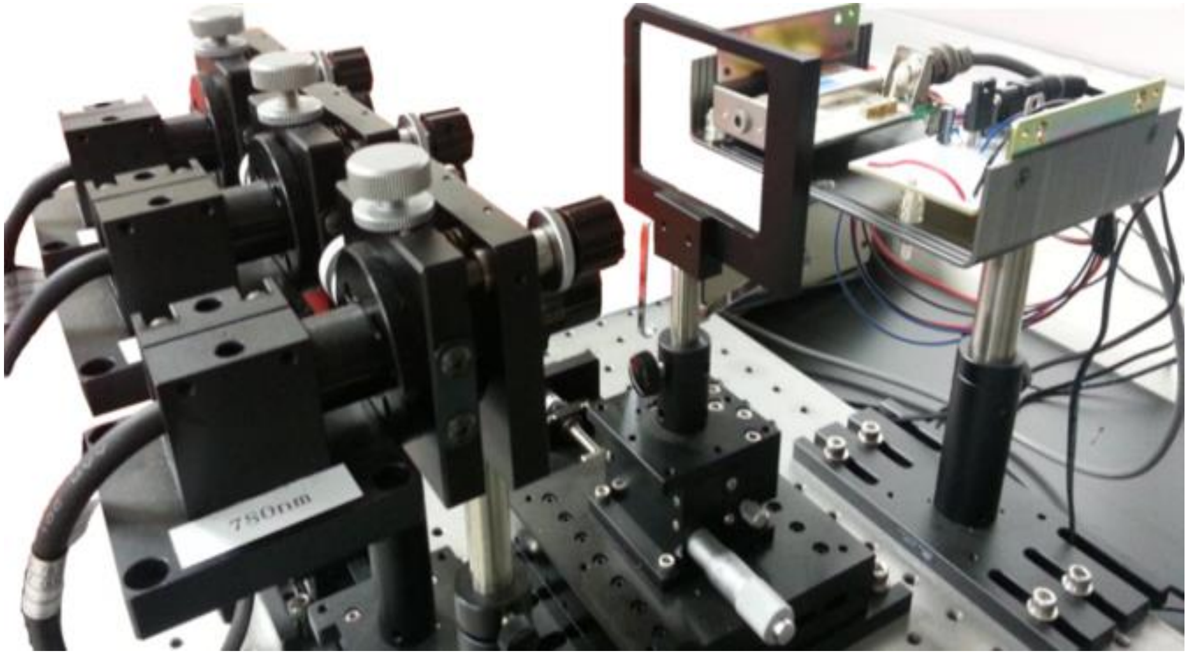

Light Sensing Technique for Detection of Wood Density

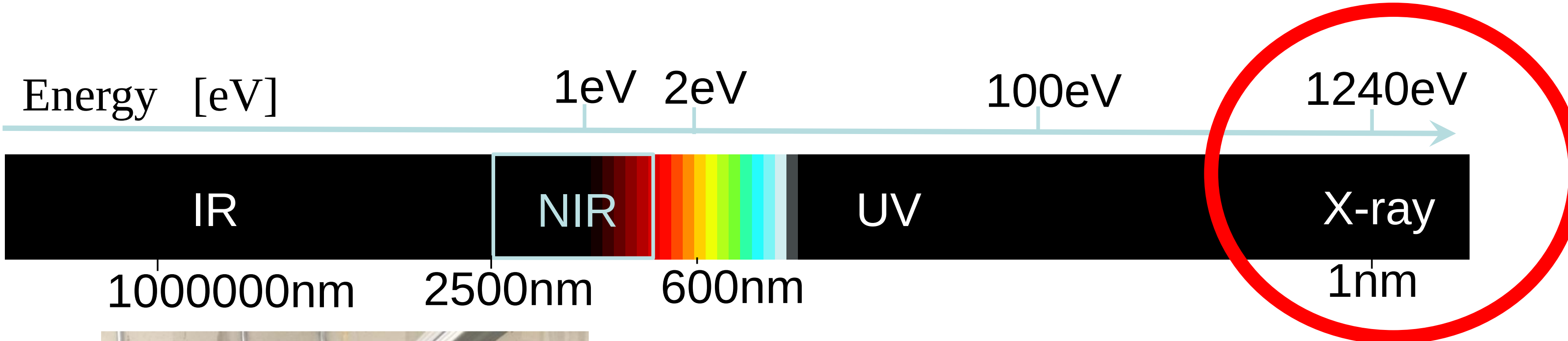

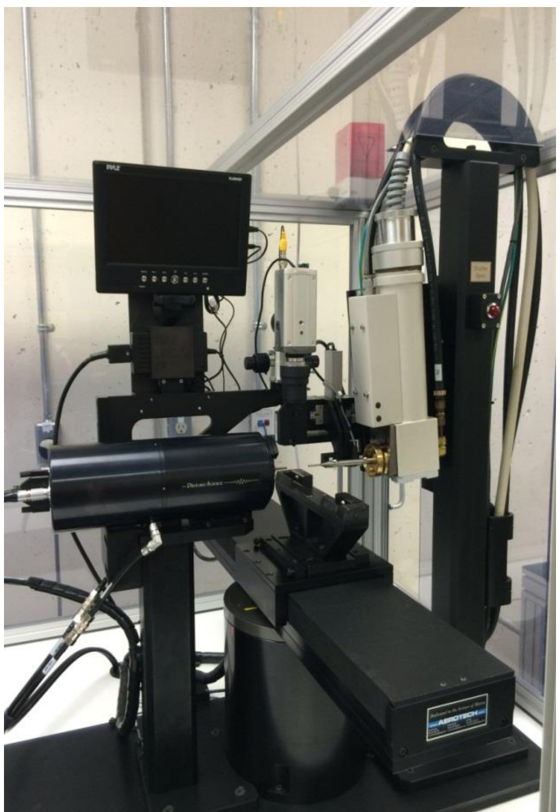

X-ray
Densitometry

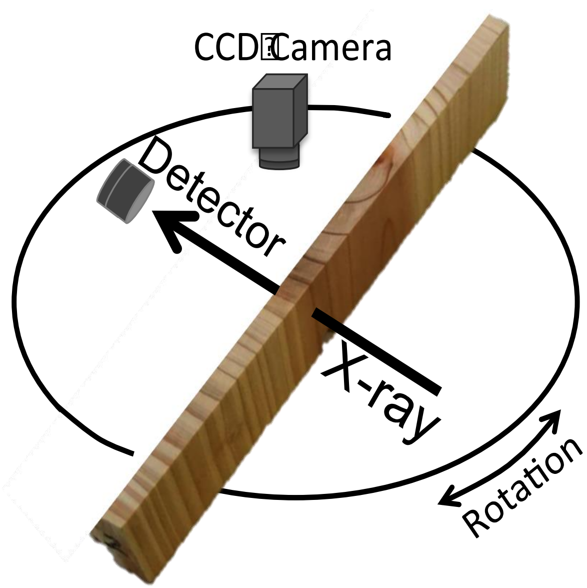

Light Sensing Technique for Detection of Wood Density

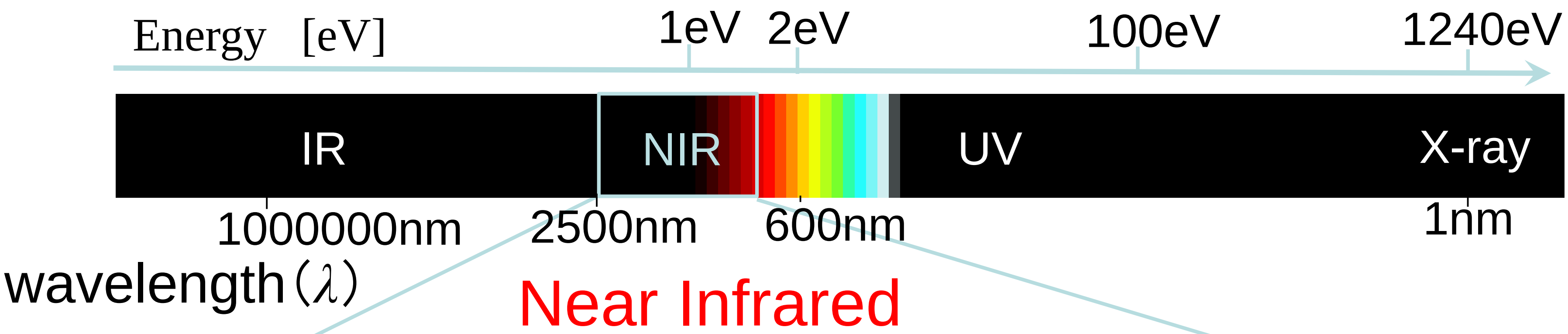

	Safety	Resolution	Cost	Coherency	Permea-bility
NIR Spectroscopy	Safely	High	Low	No	Mid
NIR Laser	**Safely**	**High**	**Low**	**Yes**	**High**

–

Development of NIR Device

- Continuous wave laser
  - Φ1mm
  - 830nm
- APD sensor
  - Φ5mm

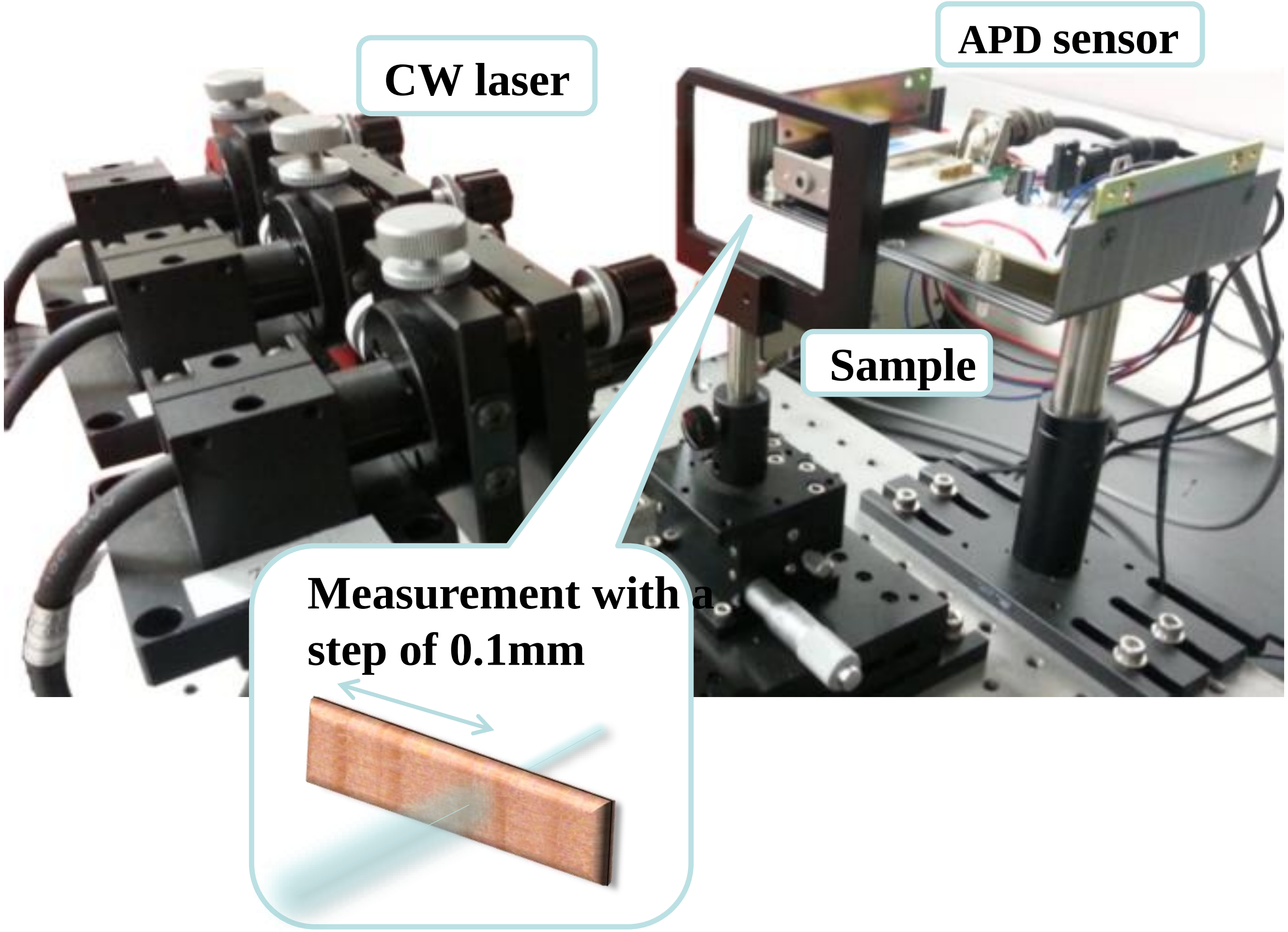

- Sample
  - Douglas fir

    (Thickness : 2mm, 3mm, 4mm)

- Measurement of density by the x-ray densitometer

  (as reference)

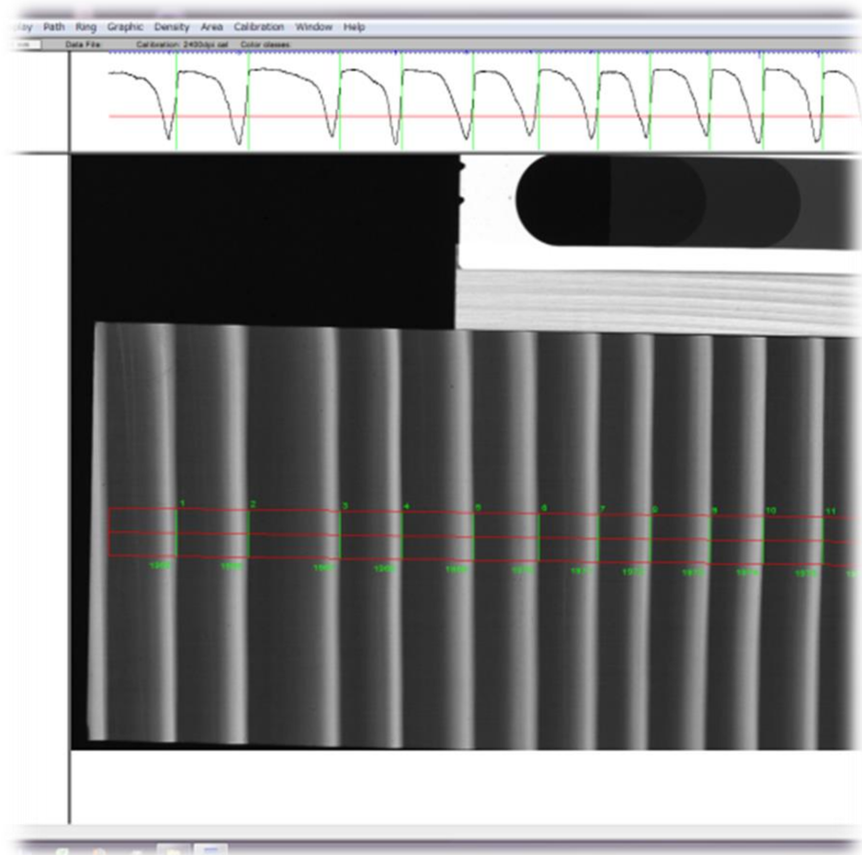

Fitting of Lambert-Beer Law

LB law is available for non-scattering materials.

$$A = \varepsilon c d$$

A : Absorbance

ε : Absorption coefficient

c : Density

d : Sample thickness

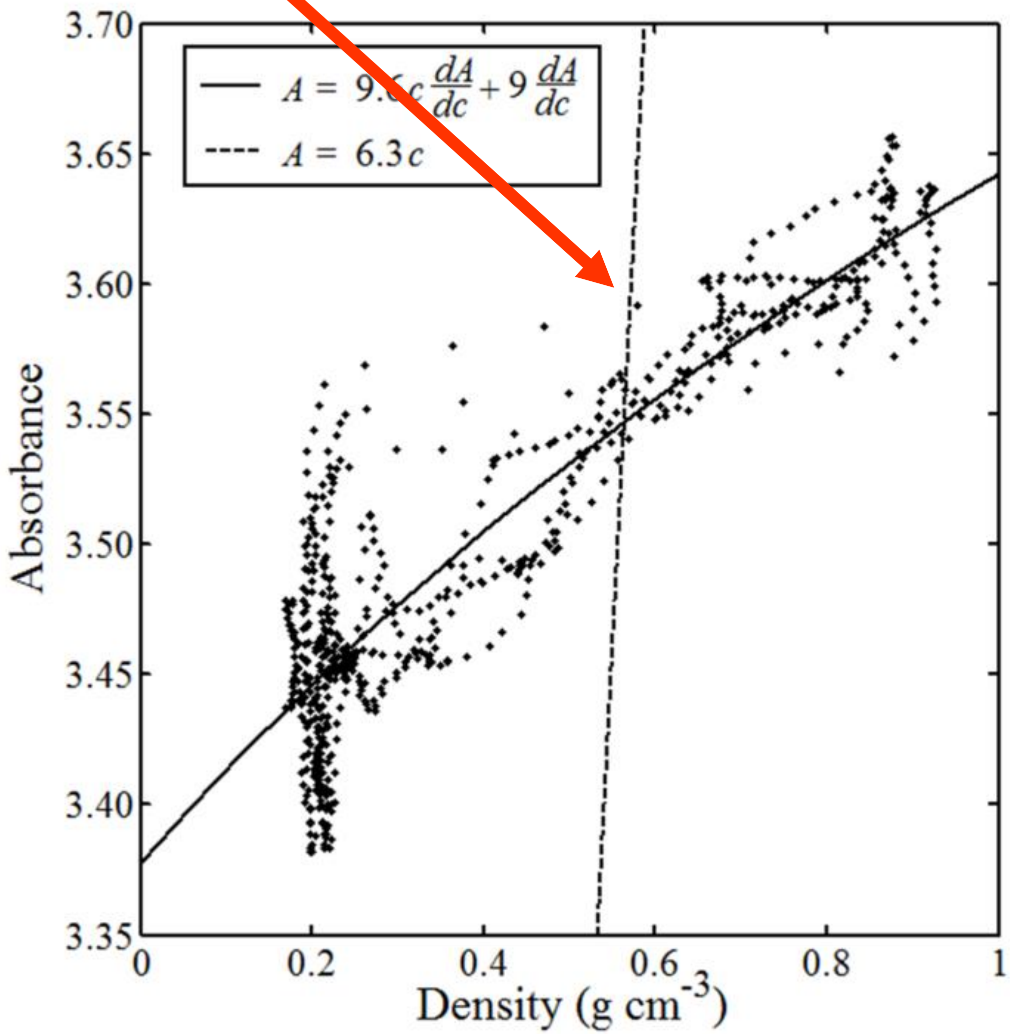

Fitting of Lambert-Beer Law

LB law is available for non-scattering materials.

$$A = \varepsilon c d$$

A : Absorbance

ε : Absorption coefficient

c : Density

d : Sample thickness

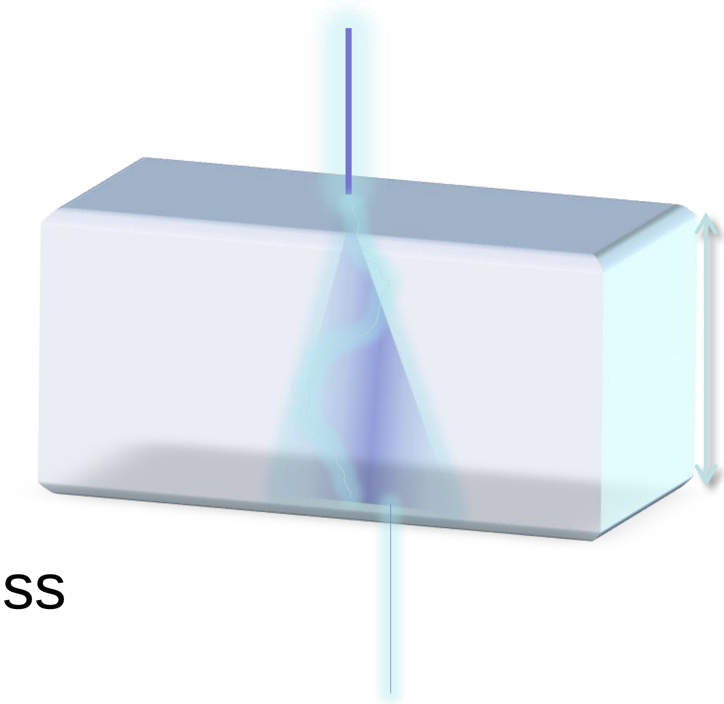

Scattering phenomenon affects optical path length.

Proposal of Modified LB Law

$$A = \varepsilon c \frac{\mathrm{d}A}{\mathrm{d}c} + G$$

A : Absorbance

ε : Absorption coefficient

c : Density

G : Attenuation

$\frac{\mathrm{d}A}{\mathrm{d}c}$: Optical path length

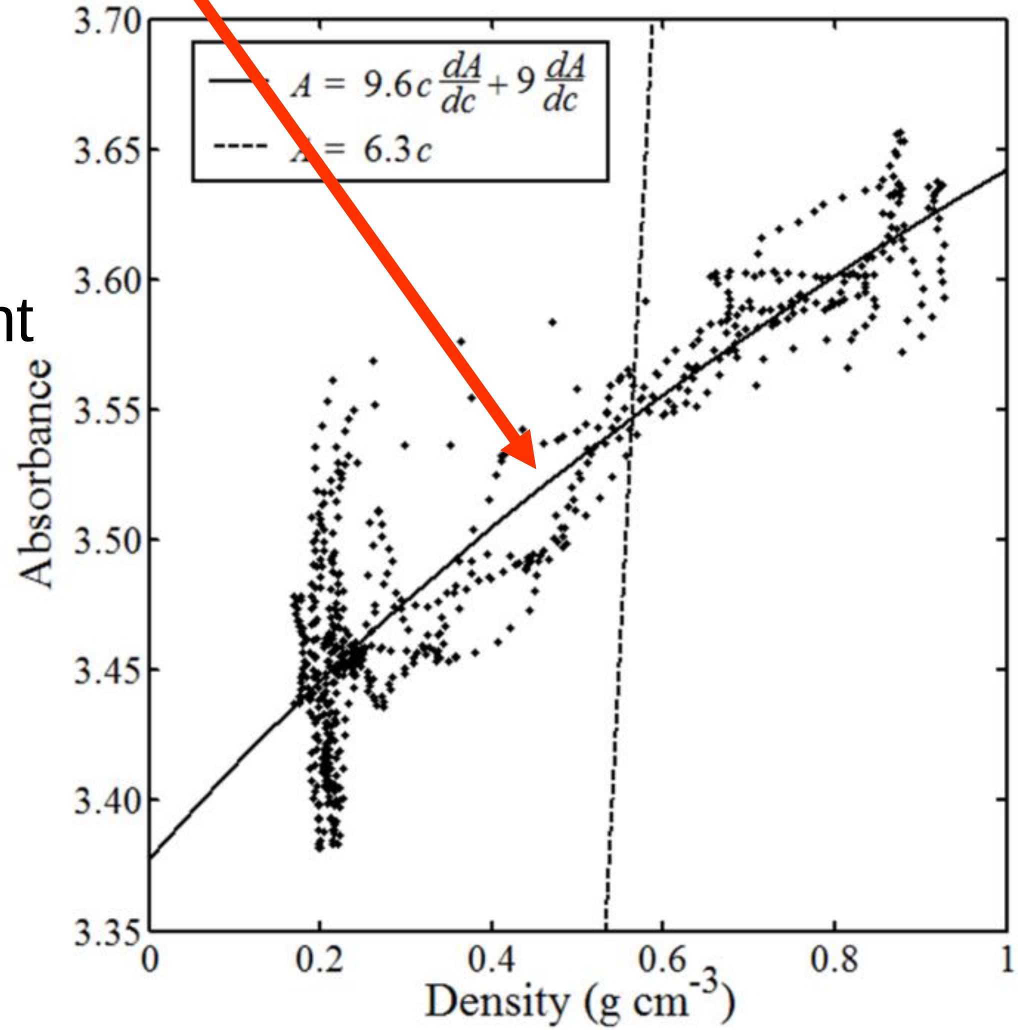

Fitting of Modified LB Law

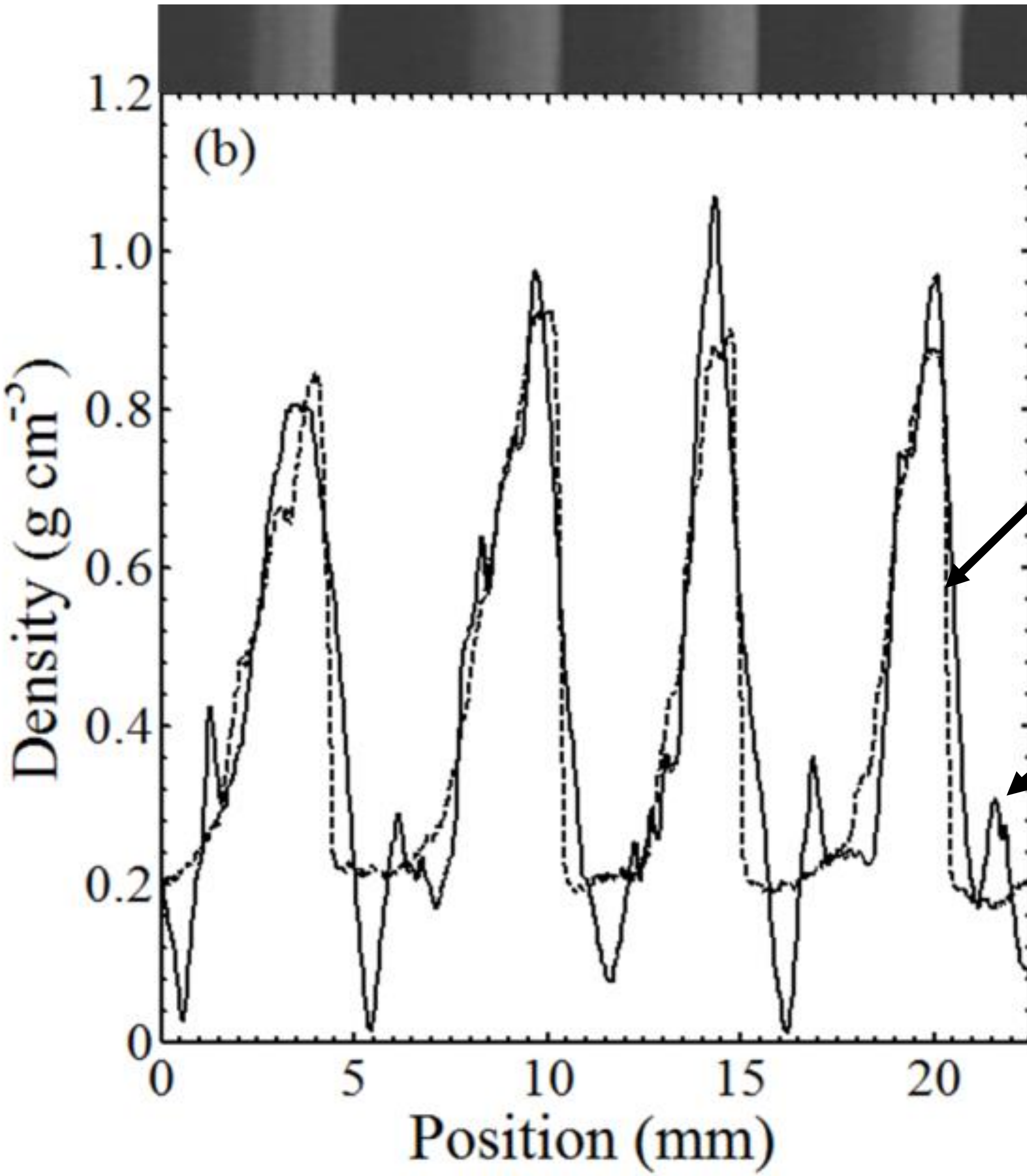

← X-ray Measurement

Measured density by X-ray device

Measured density by NIR device

Sample thickness
: 3 mm

Statistical Results due to Relationships between Measured Density by X-ray and Predicted Density by NIR

Thickness	Number of measurement points	RSS*1	R^{2}*2	RMSEC (g cm^{-3})*3
2 mm	288	0.120	0.75	0.075
3 mm	668	0.611	0.81	0.081
4 mm	295	0.175	0.73	0.105

*1The residual sum of squares

*2Determinant coefficient

*3Root mean squared error of calibration

Topic II

Determination of True Optical Absorption and Scattering Coefficient of Wooden Cell Wall Substance by Time-of-Flight NIR Spectroscopy

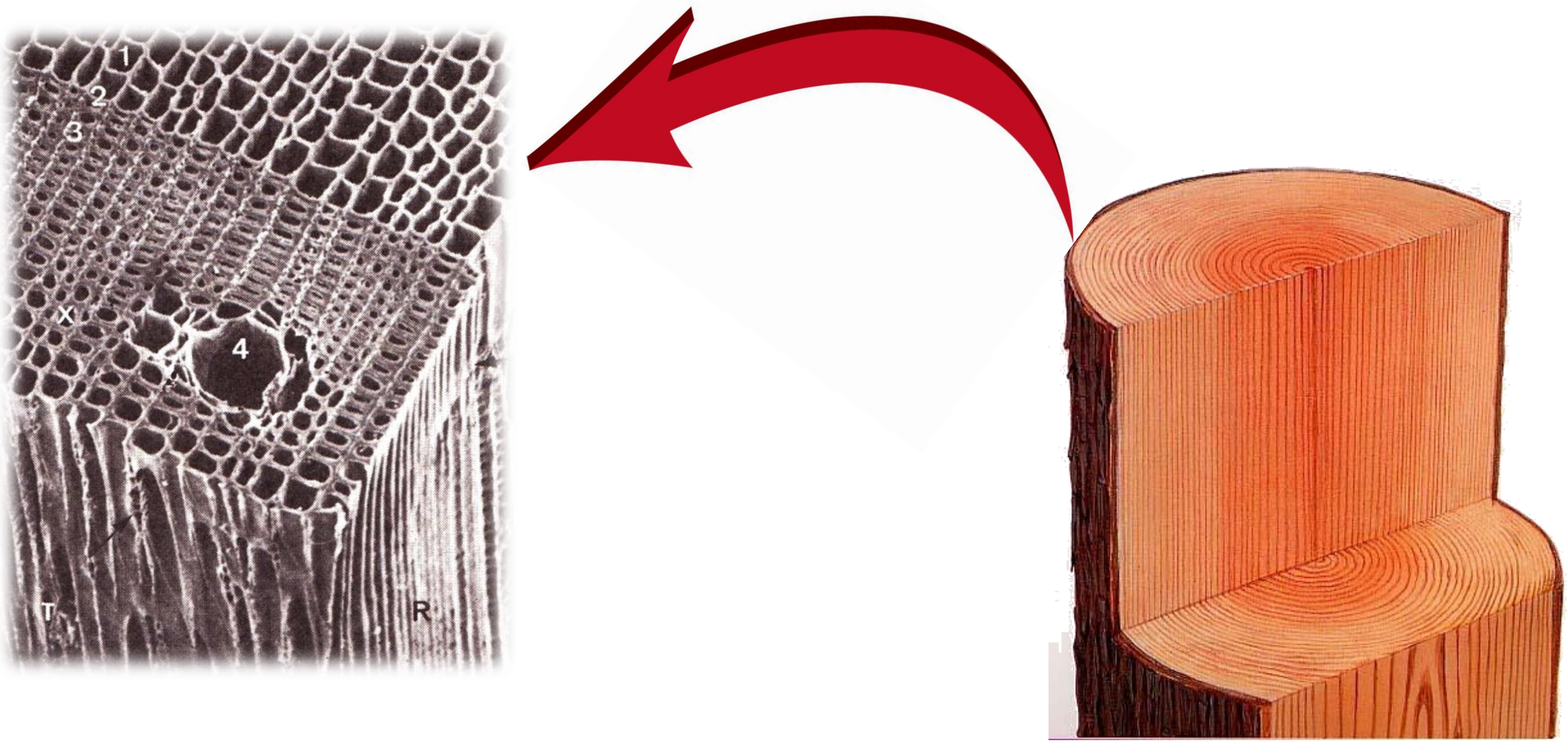

Time-of-Flight near infrared spectroscopy (TOF-NIRS) make it possible to assess the internal properties by analyzing the transmitted pulse including the information about the light propagation in sample.

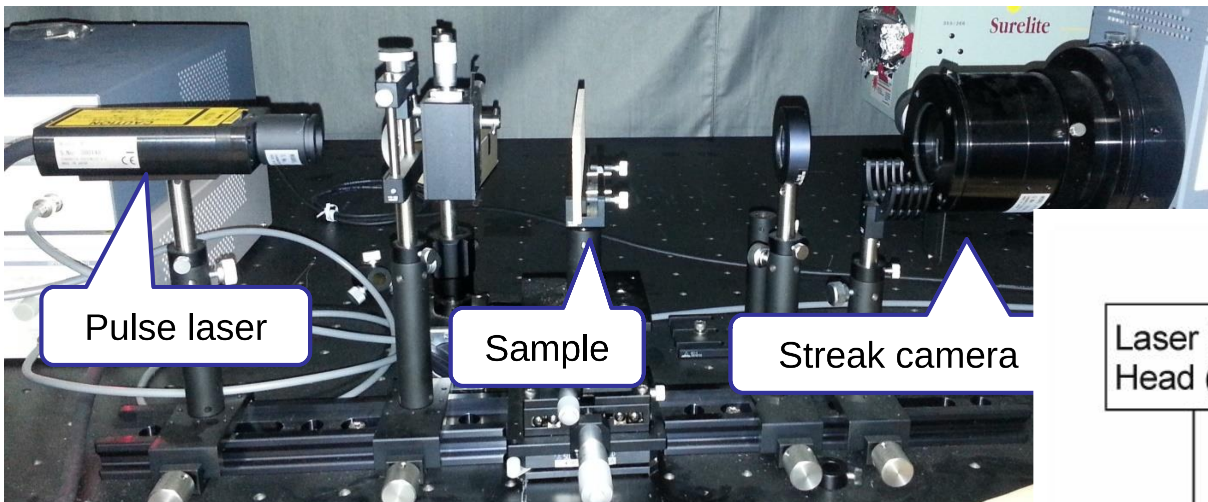

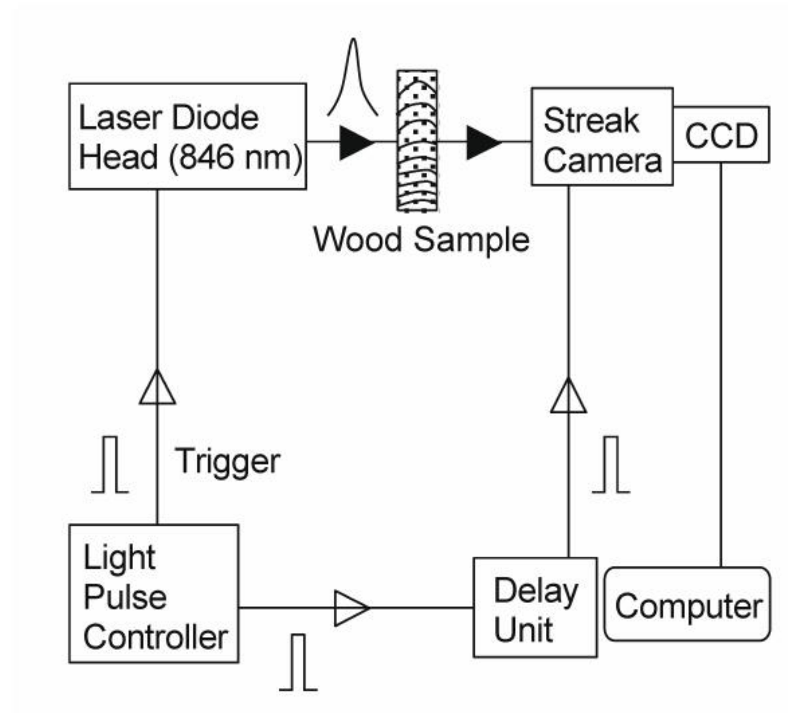

The principle of TOF-NIRS is to send short light pulses into a medium and to measure the time-resolved profile of the diffusely transmitted photons.

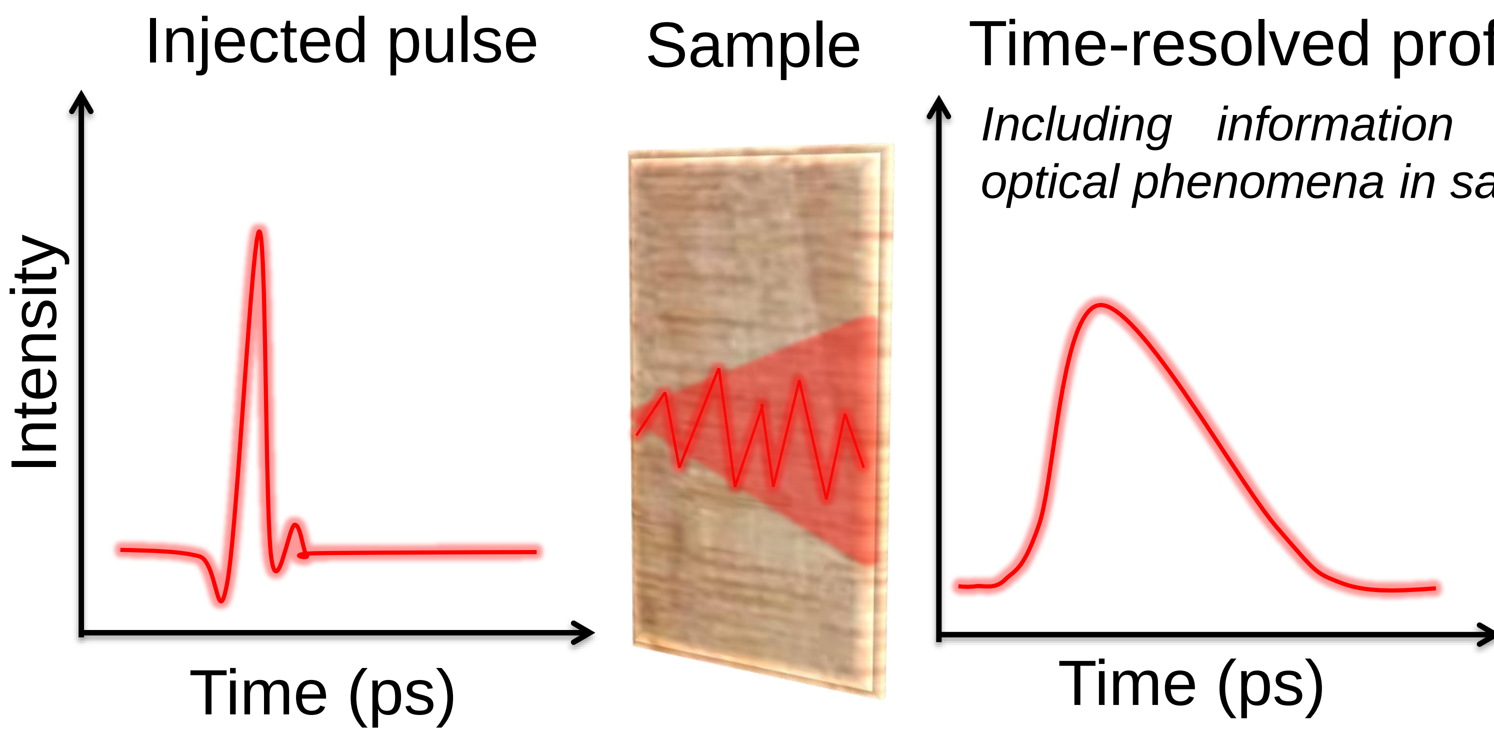

The absorption and the reduced scattering coefficients of the medium can be computed by solving the diffusion approximation to the radiative transfer equation.
(Patterson et al. 1989)

$$T(d,t)=(4\pi Dc)^{-1/2}\, t^{-3/2}\exp(\mu ct)\times\left\{(d-z_0)\exp\left[-\frac{(d-z_0)^2}{4Dct}\right]-(d+z_0)\exp\left[-\frac{(d+z_0)^2}{4Dct}\right]\right.$$
$$\left.+(3d-z_0)\exp\left[-\frac{(3d-z_0)^2}{4Dct}\right]-(3d+z_0)\exp\left[-\frac{(3d+z_0)^2}{4Dct}\right]\right\}$$

$T(d,t)$: time-resolved profile at each time, d: thickness, t: time, c: light speed (300mm/ns)
μs: reduced scattering coefficient, μa: absorption coefficient, g: anisotropic parameter
$D = [\,3(\mu s + \mu a)\,]^{-1}$, $z_0 = \mu s^{-1}$

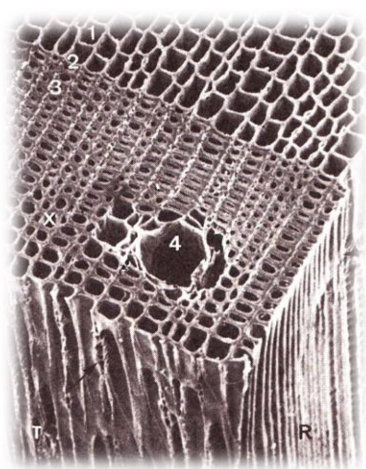

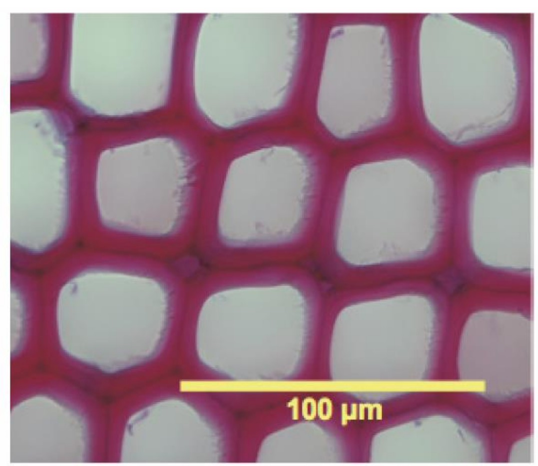

However, wood cellular structure is like aggregate of hollow fiber!!

The wood samples were impregnated with three kind of organic solvent to reduce multiple scattering in lumen.

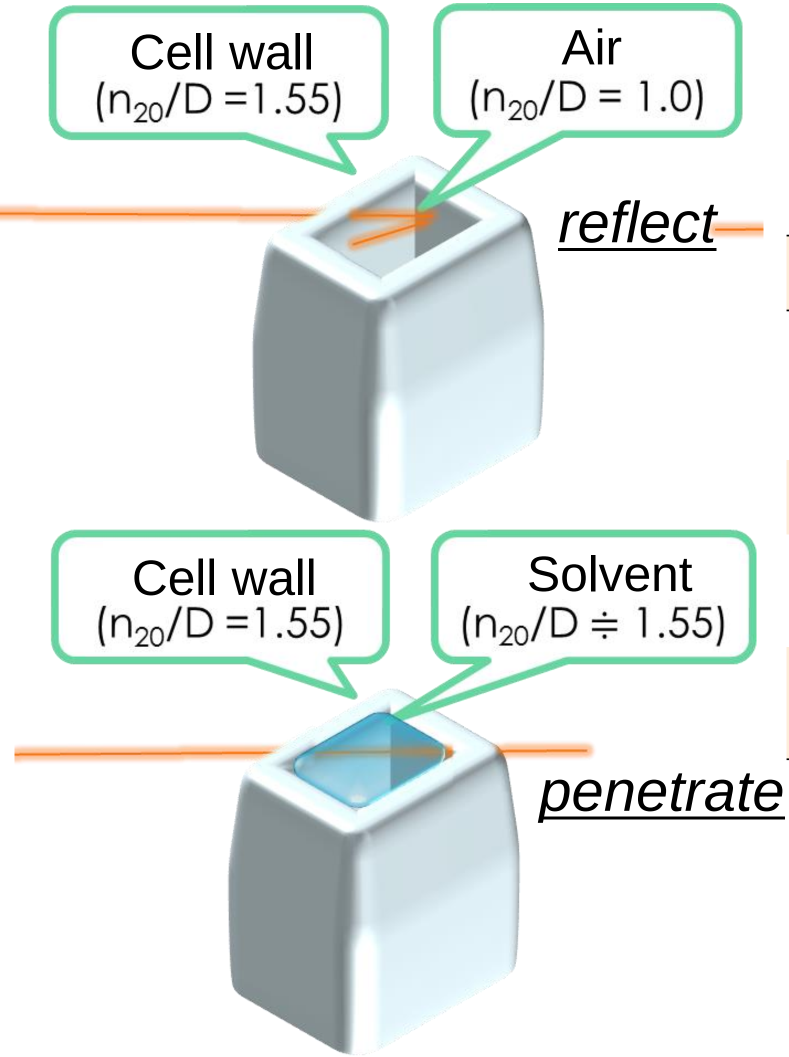

	Hexane	Toluene	Quinoline
Chemical formula	C_6H_{12} 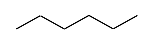	$C_6H_5CH_3$ 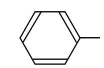	C_9H_7N 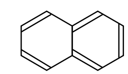
Density (g/cm^3)	0.692	0.8623	1.093
Refractive index (n_{20}/D)	1.388	1.4969	1.625
Absorption coefficient (/mm)	0.00129	0.05957	0.00540

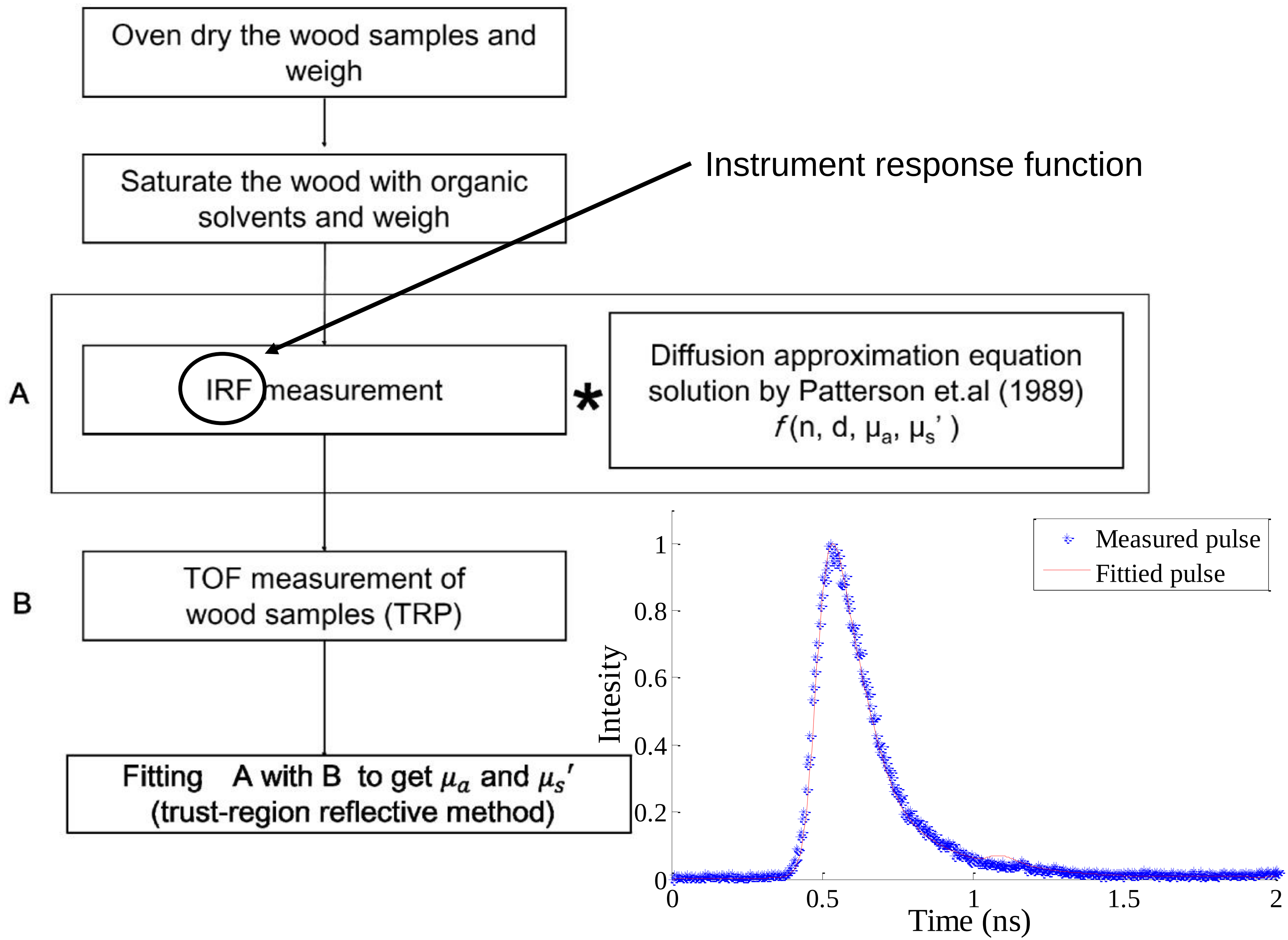

Oven dry the wood samples and weigh
Saturate the wood with organic solvents and weigh
Instrument response function
A
IRF measurement
*
Diffusion approximation equation solution by Patterson et.al (1989)
$f(n, d, \mu_a, \mu_s')$
B
TOF measurement of wood samples (TRP)
Fitting A with B to get μ_a and μ_s' (trust-region reflective method)
Measured pulse
Fittied pulse
Intesity
Time (ns)
0
0.2
0.4
0.6
0.8
1
0
0.5
1
1.5
2

Simulation based on Monte-Carlo method, which can describe light diffusion in complex material by computing with random numbers

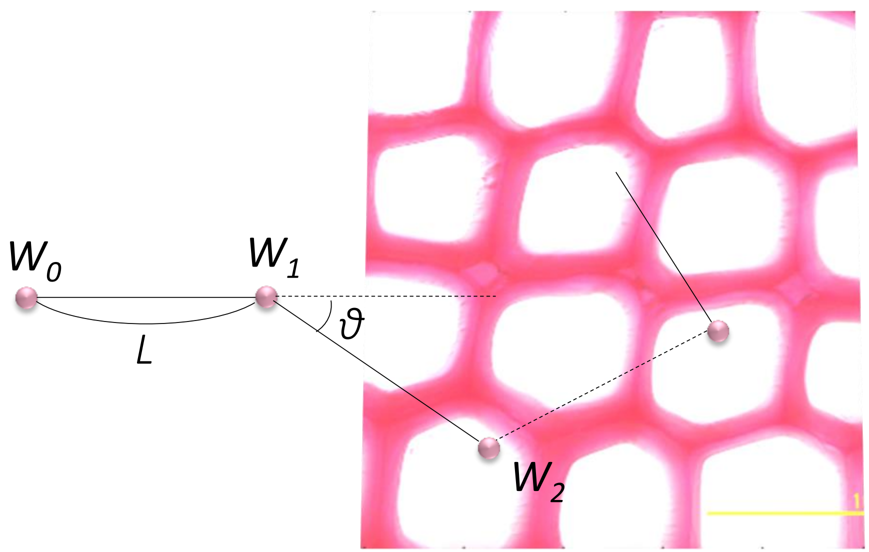

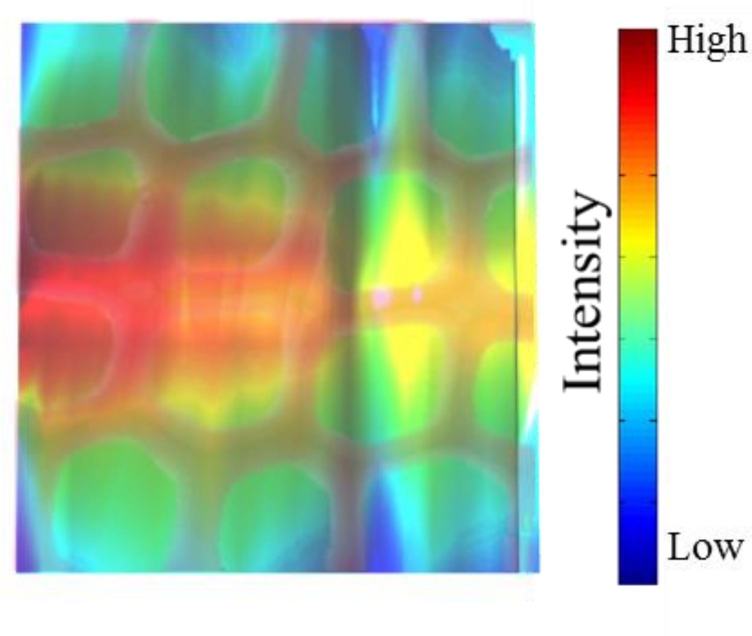

Step length: $L = -\ln(R_1) / \mu_t$
Scattering angle: $\theta = 2\pi R_2$
Decision of scattering: $R_3 \leqq \mu_t / \mu_{tmax}$
Decision of absorption: $W_{i+1} = W_i * \mu_s / \mu_t$

μ_s: Scattering coefficient
μ_a: Absorption coefficient
μ_t: Attenuation coefficient
R: Random number
W: Weighting factor

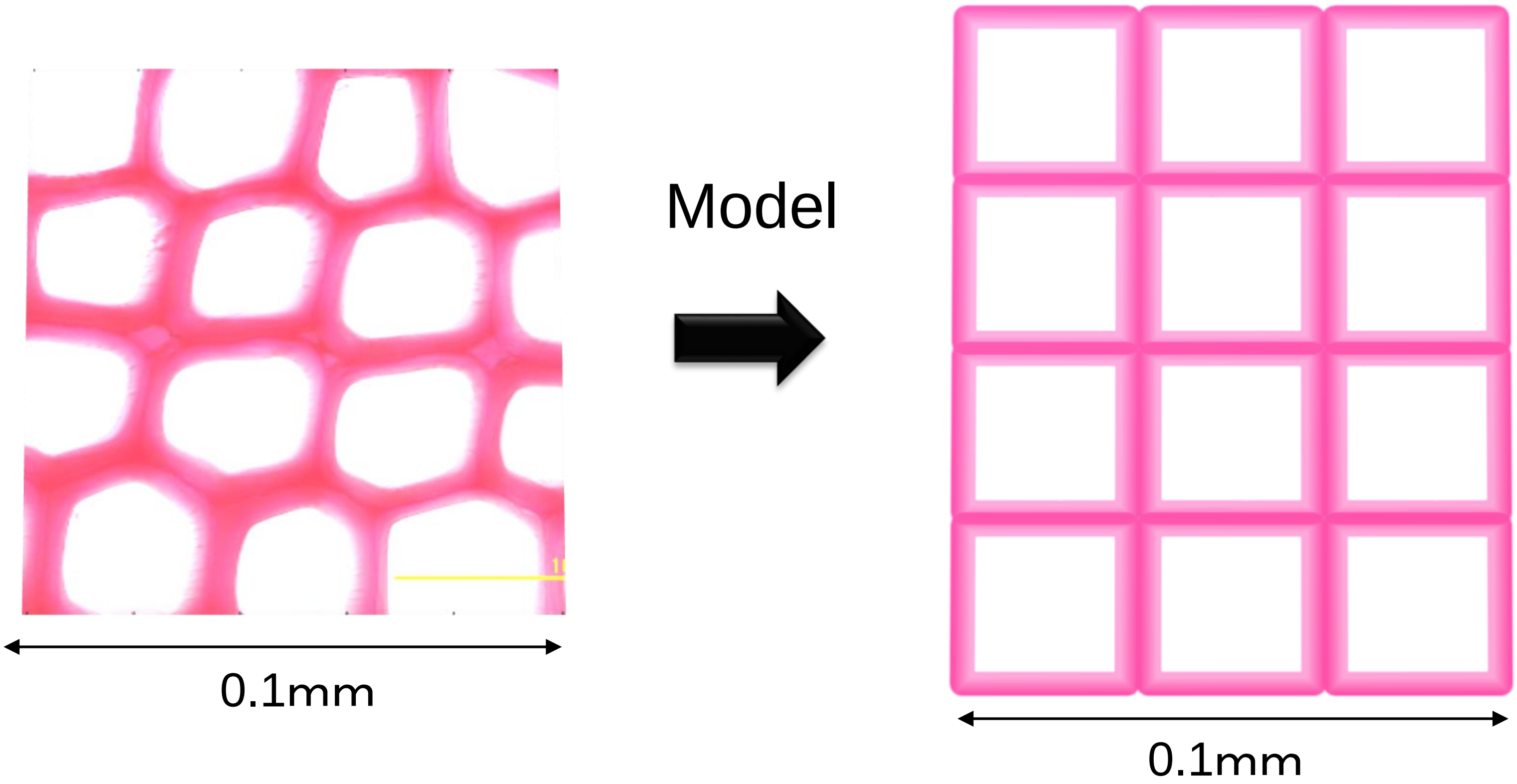
Model
0.1mm
0.1mm

Time-Resolved Profile Obtained from Dry and Impregnated Wood Sample

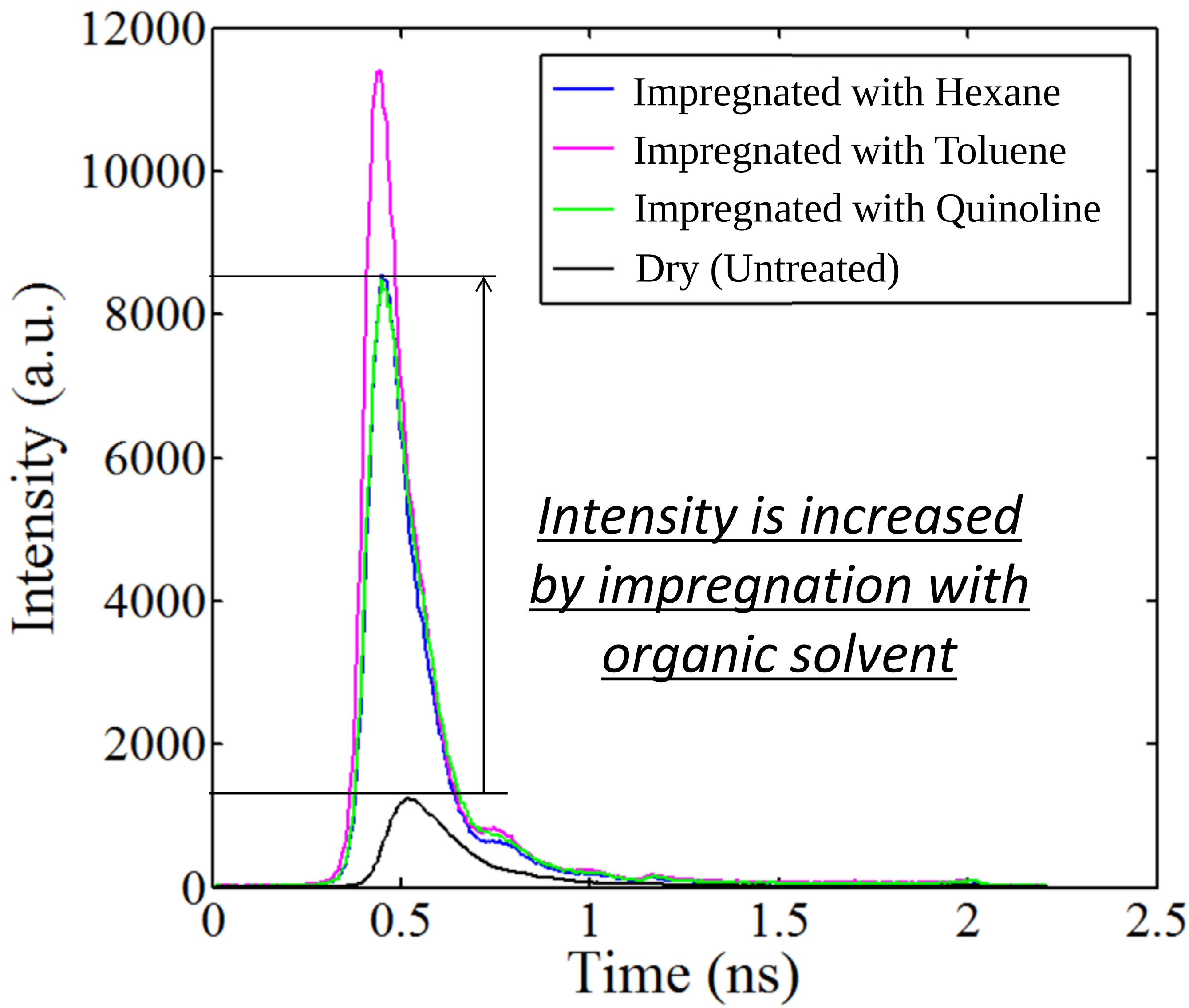

Relationship between Refractive Index of Impregnating Material and Average Pathlength

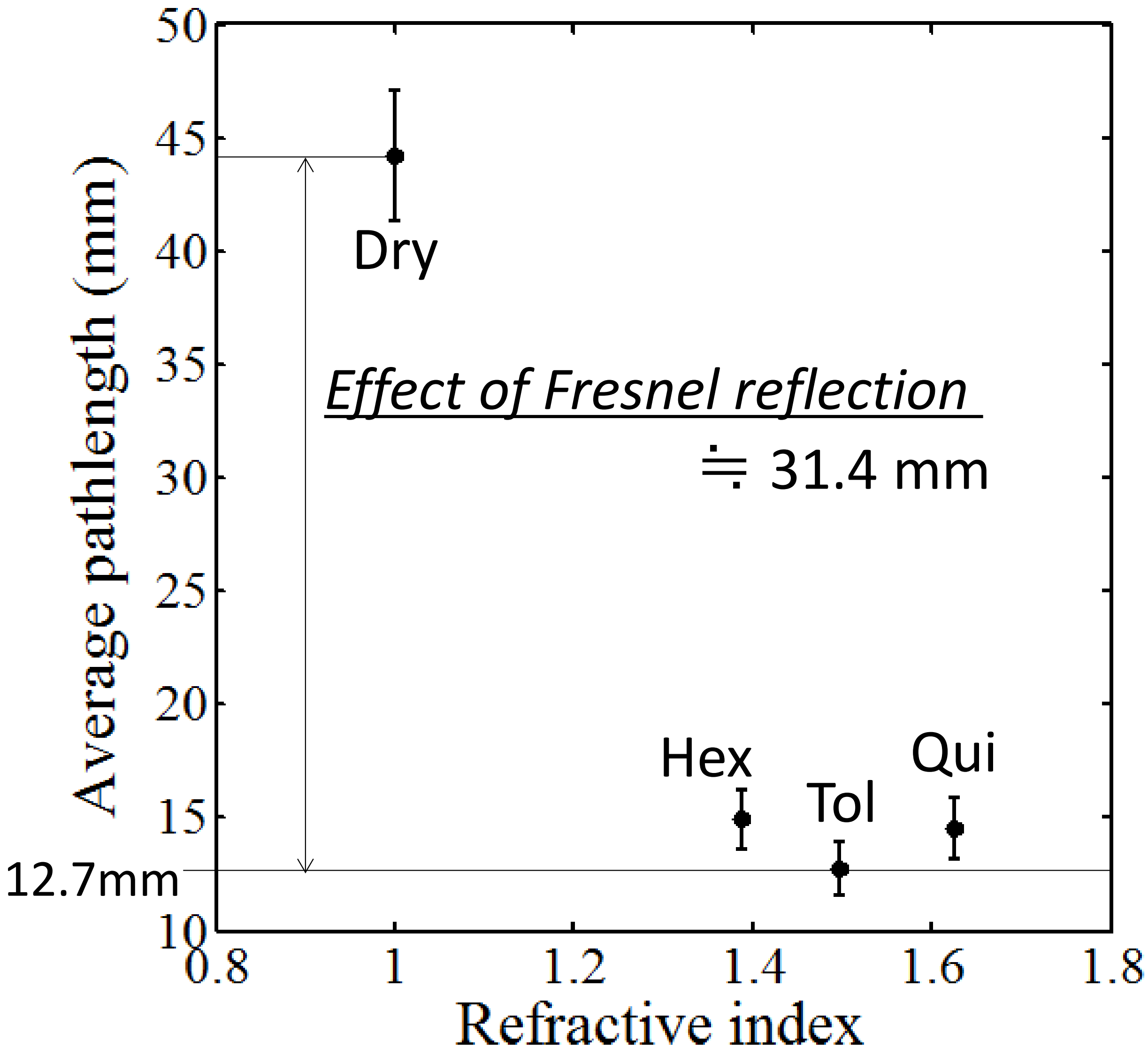

Relationship between Refractive Index of Impregnating Material and Reduced Scattering Coefficient or Absorption Coefficient

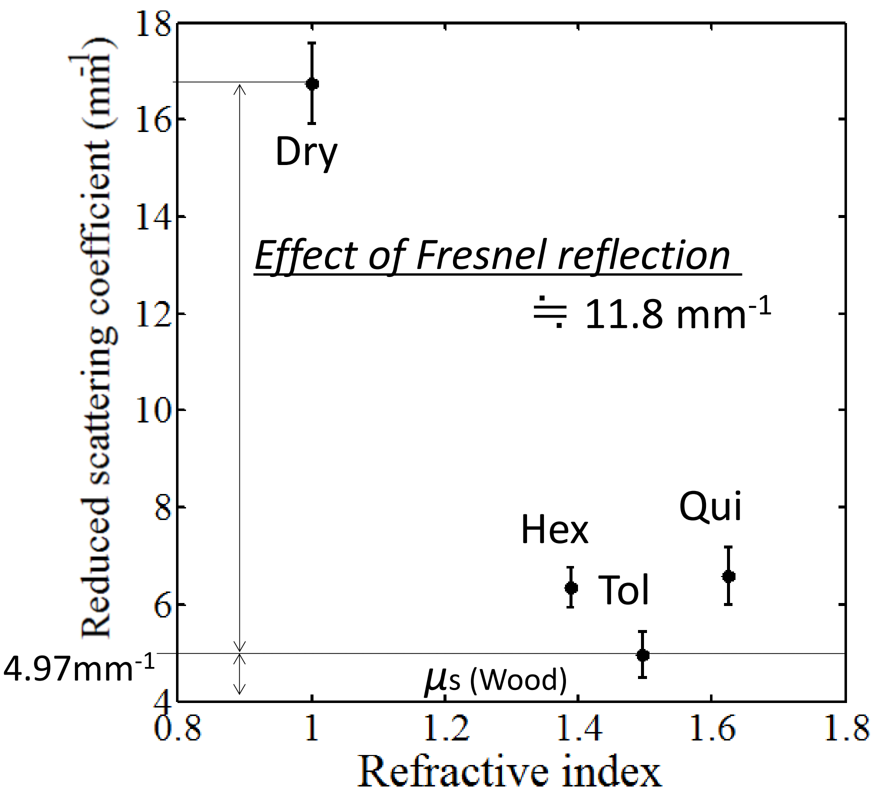

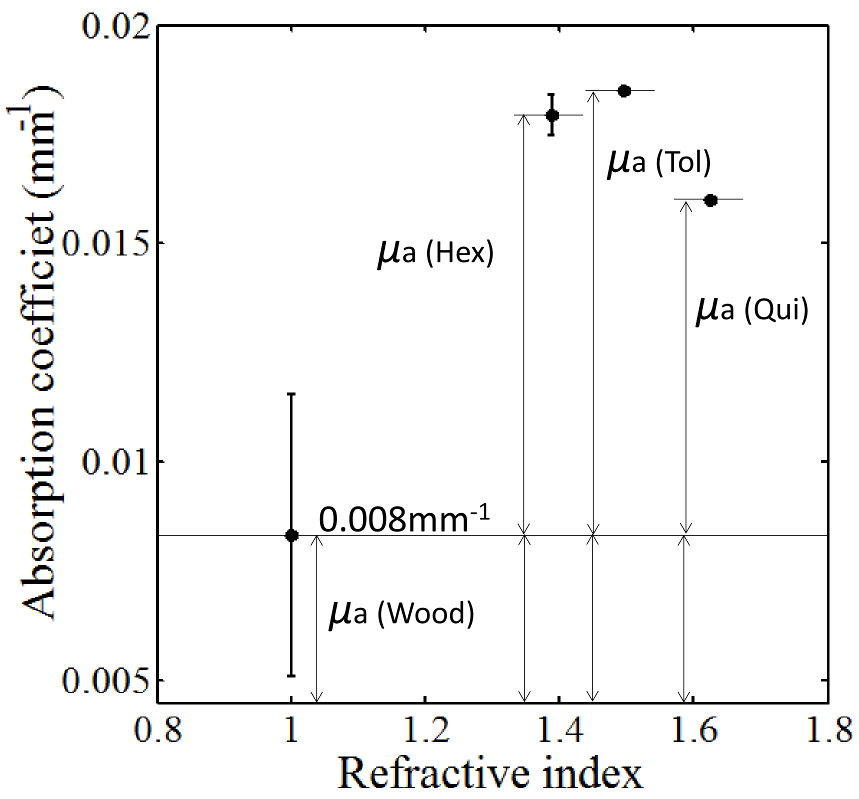

Comparison between Measured Profile with TOF-NIRS and Simulated Profile with Monte-Carlo Simulation

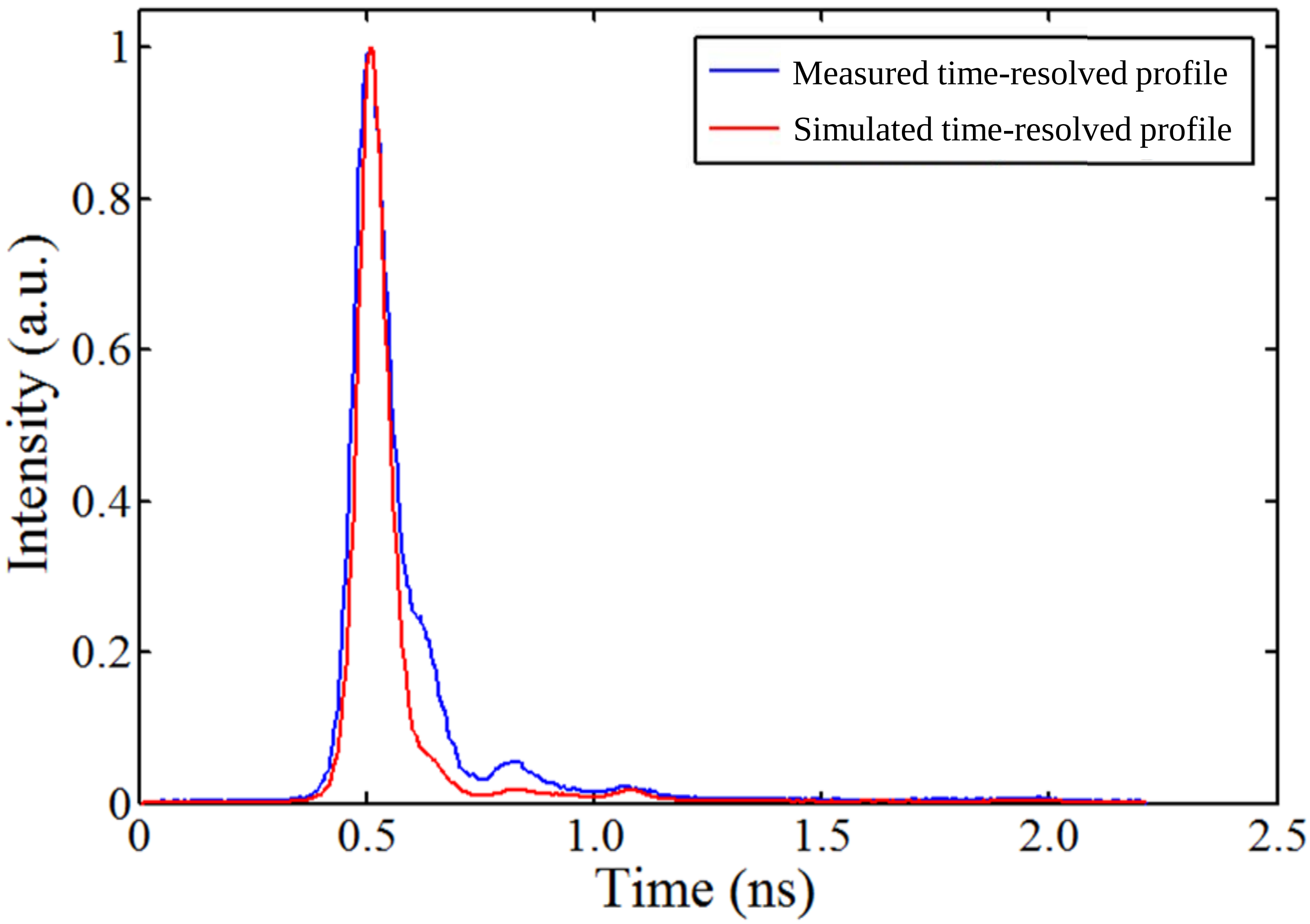

Reduc… scattering (μ_s) and absorption (μ_a) coefficient of wood … were **18.4** mm^{-1} and **0.030** mm^{-1}, respectively.

There is nothing such as absorption !

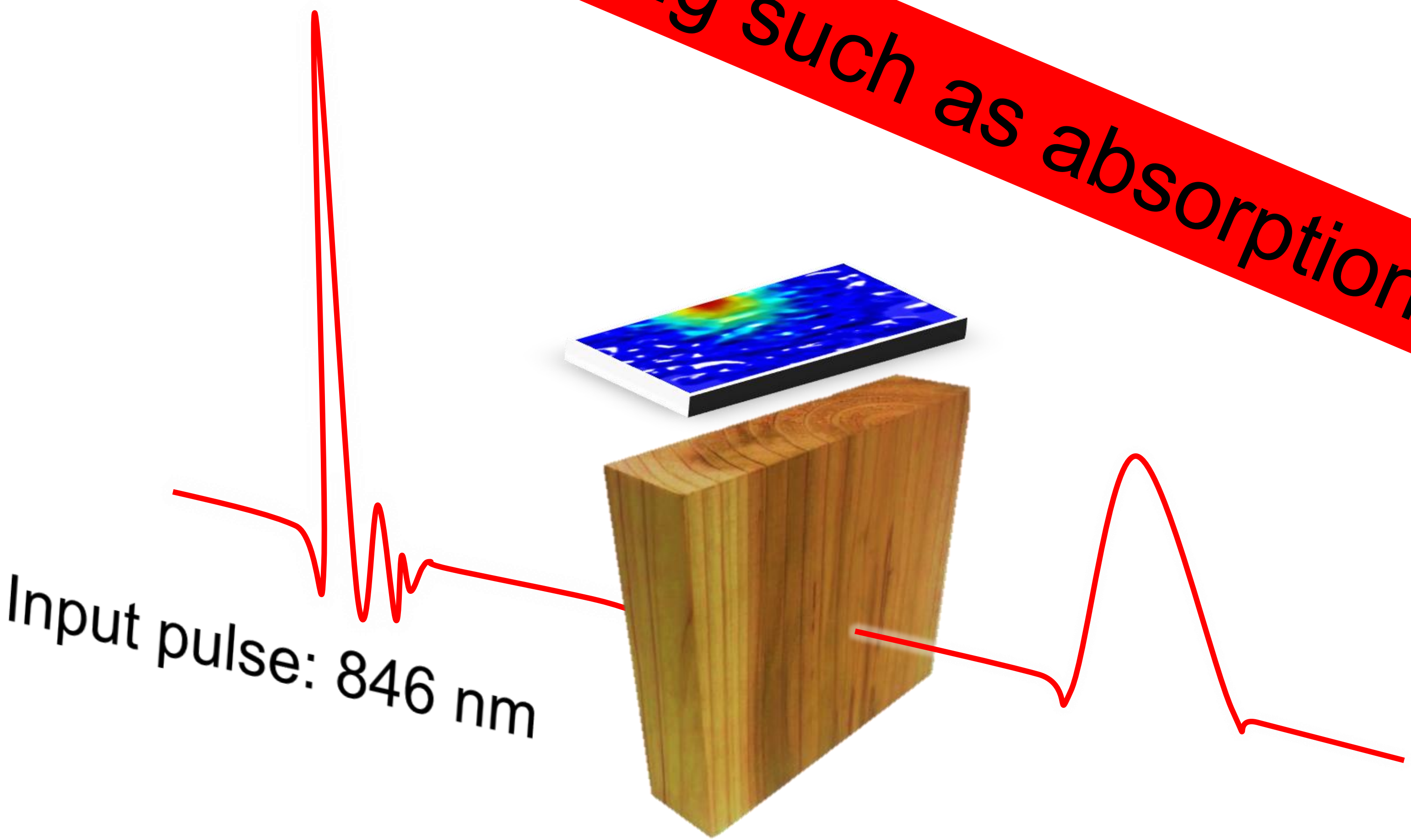

Topic III

Optical Properties of Drying Wood Studied by TOF-NIRS

Measurement of TRP of Wood at Various Moisture Content

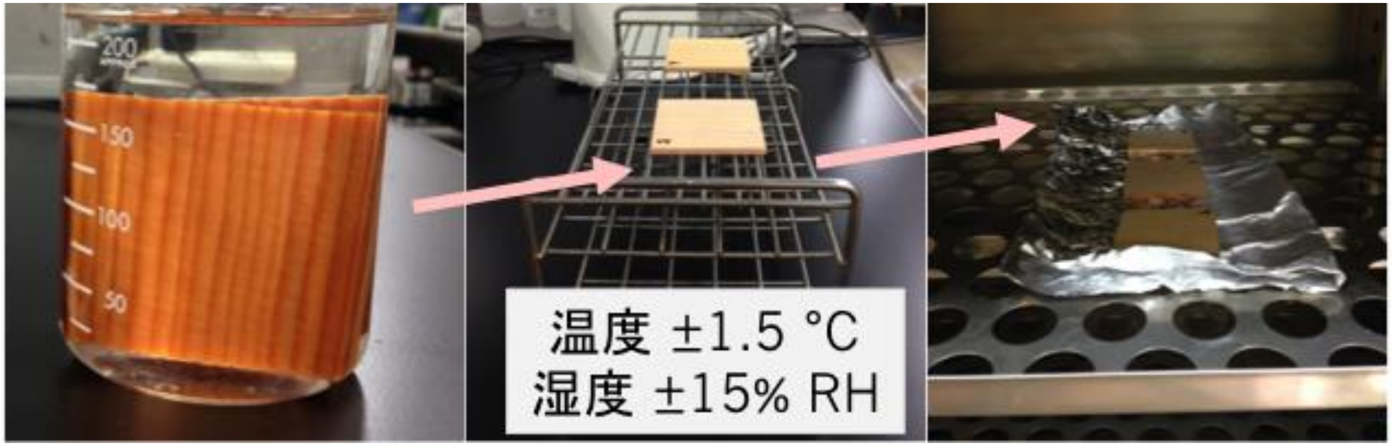

Examples of measured photon time-of-flight distributions at wavelength of 846 nm for the wood samples with moisture content (MC) of about 12% (air-dried), 30% (fiber saturation point) and 120% (water saturated)

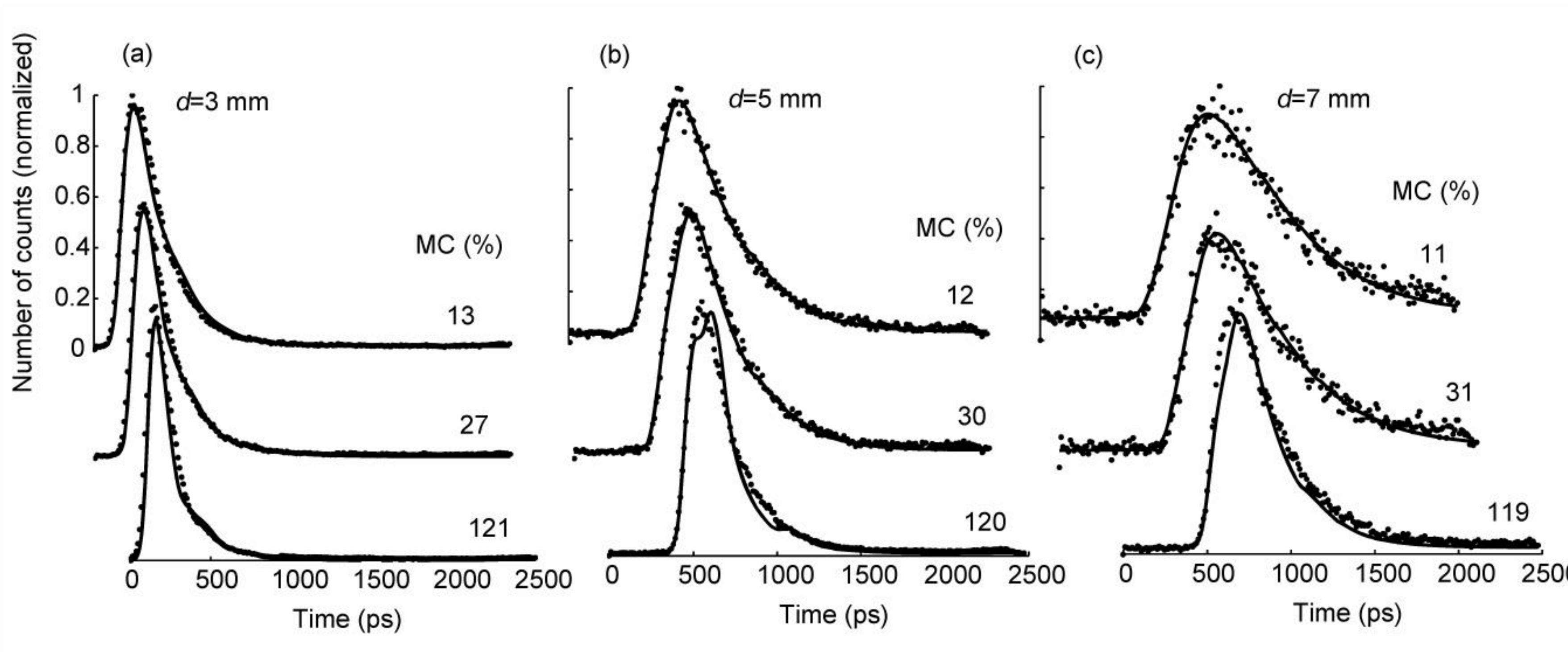

As the wood dries, the photon distribution became broader, resulting in the increase of reduced scattering (μ_s'). In the falling edge, the slope became gentler, resulting in the decrease of optical absorption (μ_a).

Changes of Reduced Scattering Coefficients during Drying of Wood

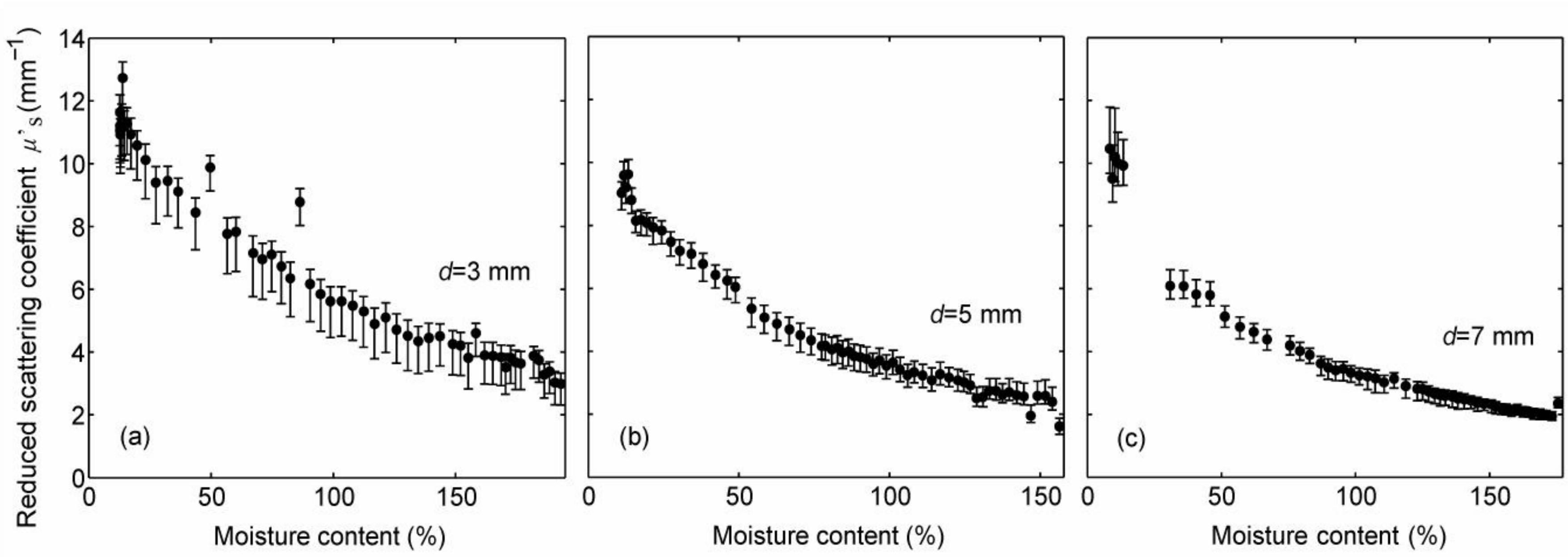

As the wood dries, the isotropic scattering event per unit length increased. The independence of values on the sample thickness ensure the robust calculation.

Characteristic Changes of Drying Rate Ratio (open square) and Reduced Scattering Coefficient (filled circle)

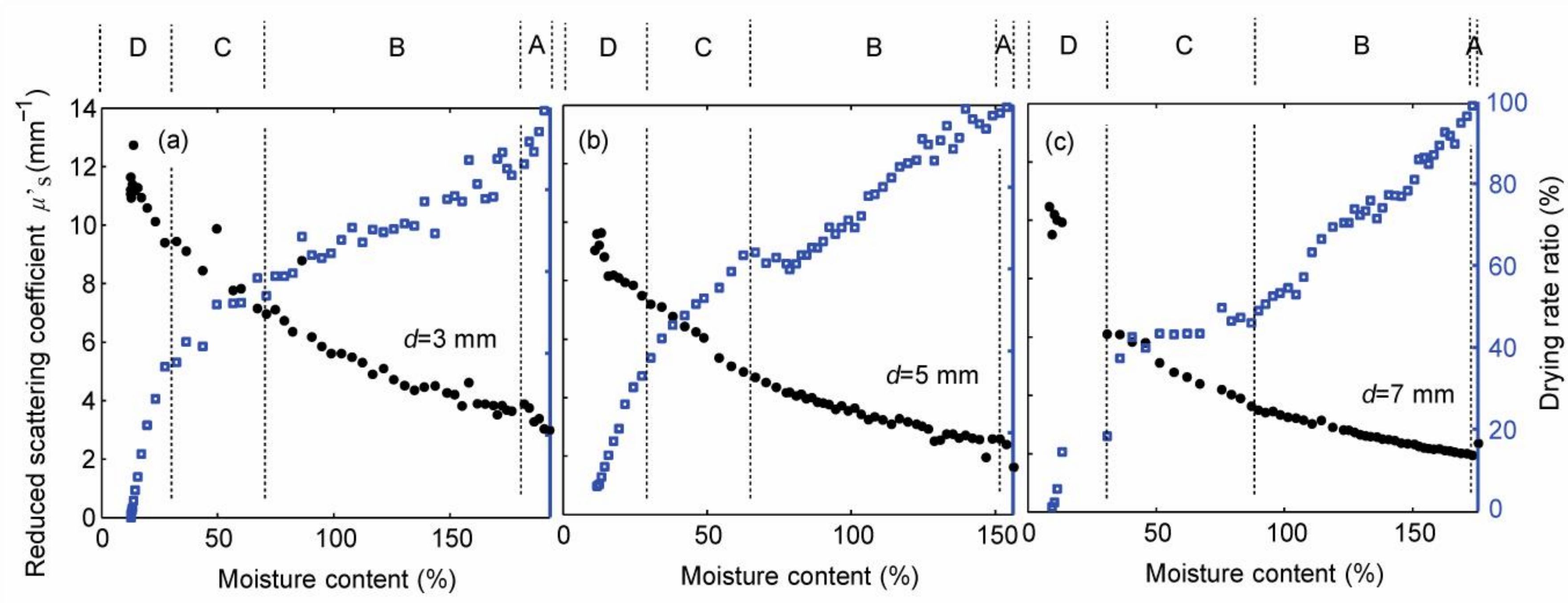

Four drying phases were estimated based on the change of the drying rate curve; constant rate period (Phase A), an early part of 1st falling rate period (Phase B), a late part of 1st falling rate period (Phase C) and 2nd falling rate period (Phase D). As the drying phase changes, the reduced scattering (μ_s') changed more radically.

Fluctuations of Surface Temperature (open square) and the Change of (a) Drying Rate Ratio (filled square) and (b) Reduced Scattering Coefficient (filled circle)

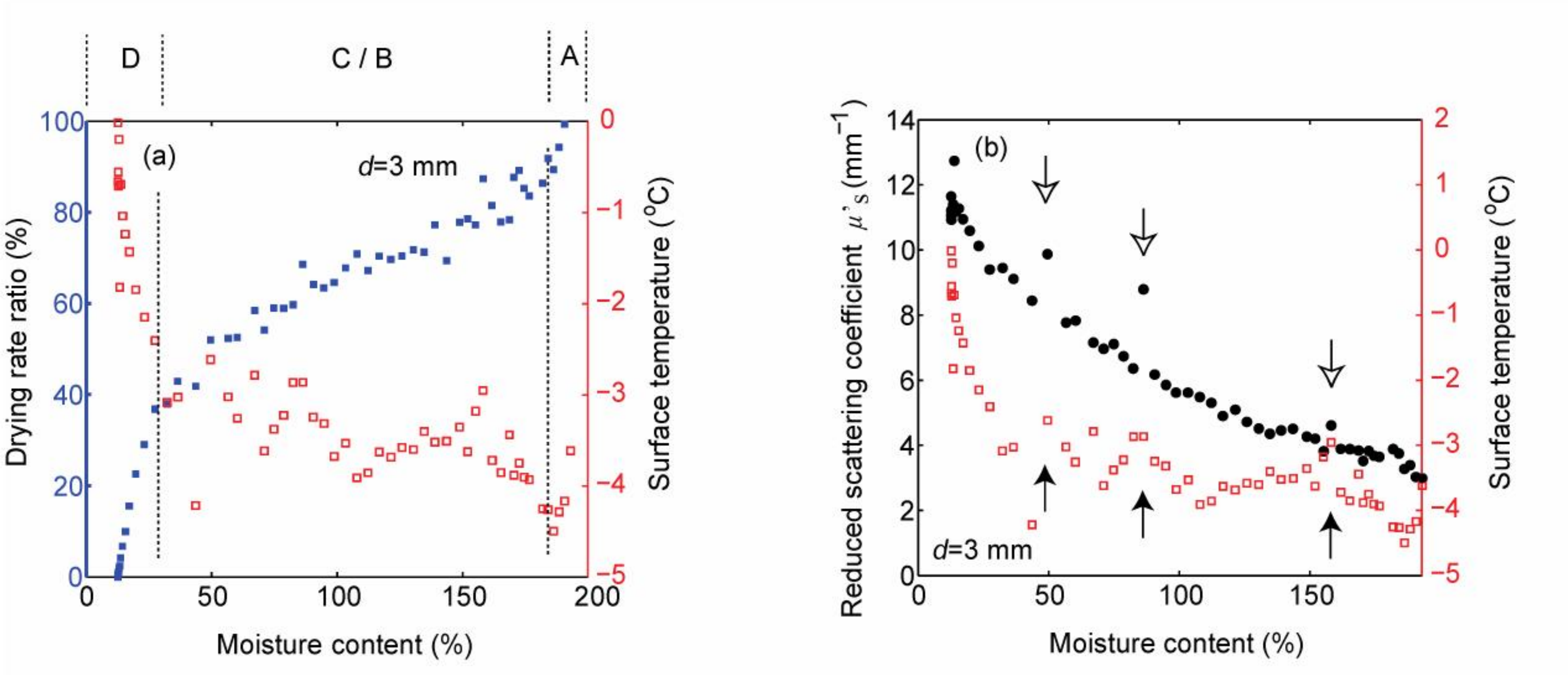

(a) Surface temperature (temperature difference between wood and air) had a negative linear relation with the drying rate ratio and increased during drying. However, surface temperature fluctuated, while the drying rate ratio changed smoothly. (b) The surface temperature jumping up indicates dry-up of the surface layer of the wood (upward arrow) and it affected the sample scattering coefficient increasing.

Changes of Optical Absorption Coefficients during Drying of Wood

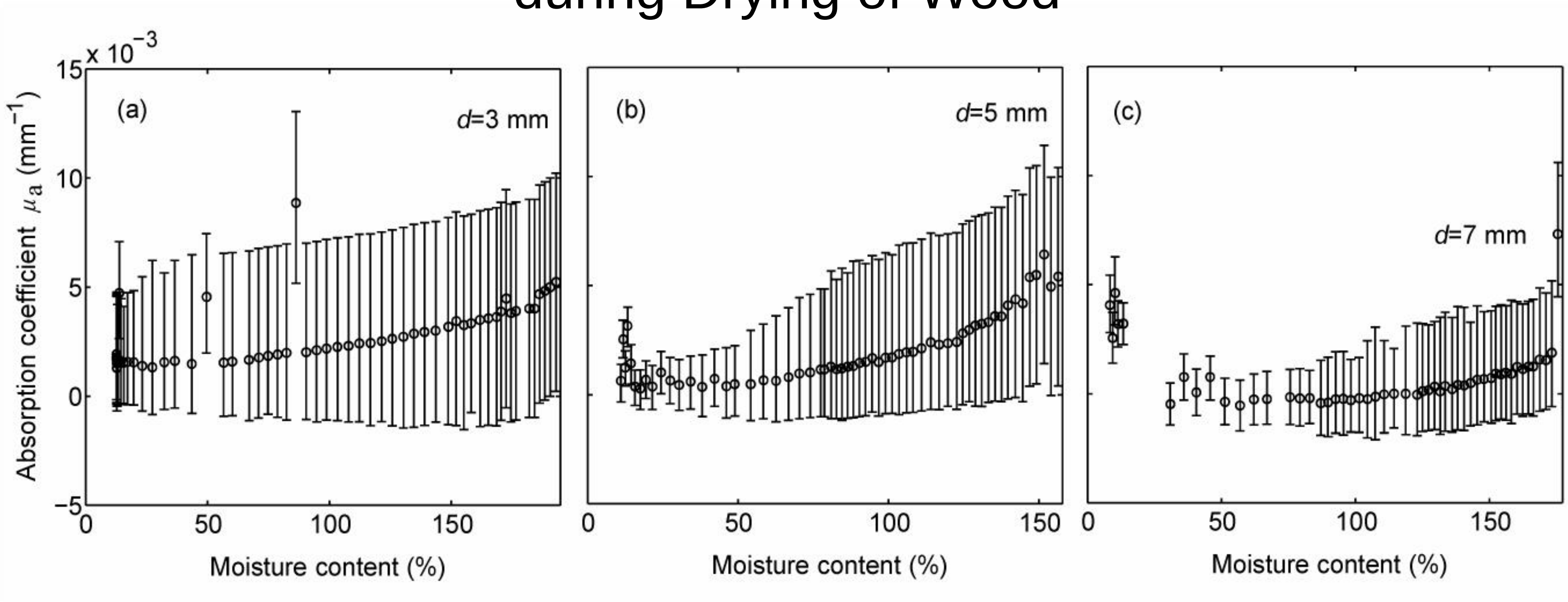

The optical absorption was found to decrease during drying of wood. The mean slope of μ_a as a function of the volume fraction of water matched well to a value of water absorption. The correspondence indicated that the absorption was derived from the absorption of water molecule which has the peak wavelength at 970 nm.

Scattering Angle Distributions for Wet (full line) and Dry (broken line) Wood

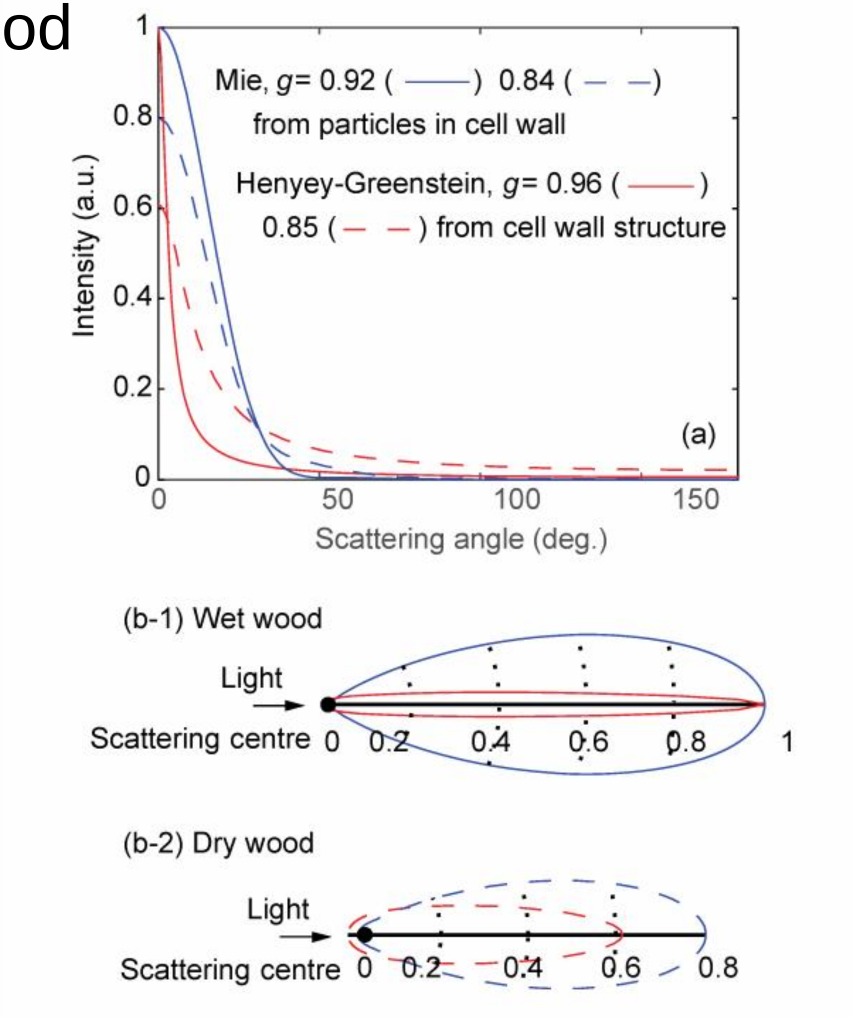

The scattering patterns from cell wall structure (red line) and the patterns from small particles in cell wall (green line) changed similarly toward the isotropic scattering by the drying effect.

Schematic Diagram of the Light Scattering on the Scale of the Tracheids (a) and of the Wood Tissue (b) in the Case of Water Saturated Condition (1) and of Low Moisture Content Condition (2)

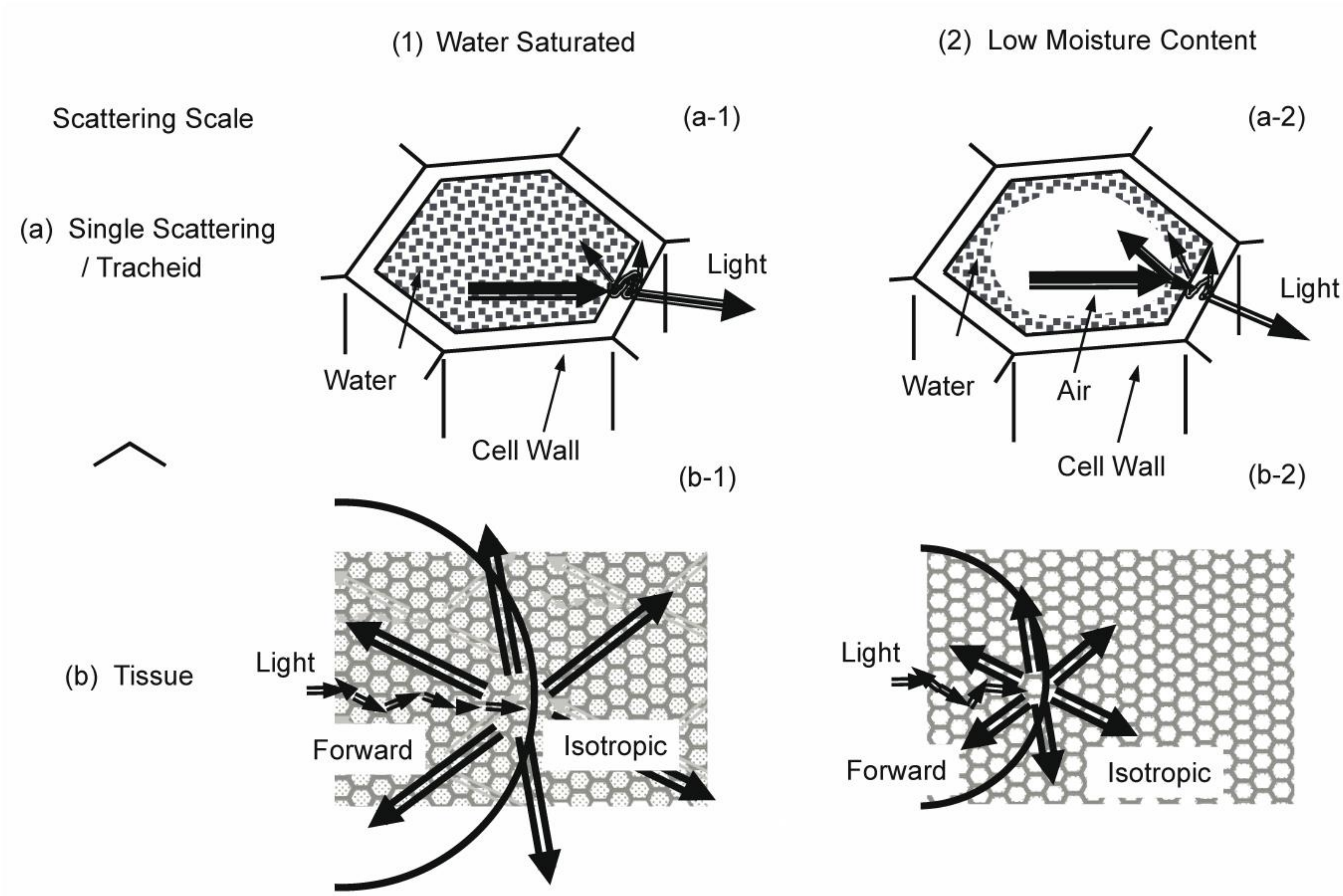

Characteristic Changes of Reduced Scattering Coefficient and the Scattering Characteristic of Pores in Wood for each Drying Phase

Drying phase	Phase in Figures	Change of reduced scattering	Lost moisture		Pore scatter theory		Scatter isotropy	
			Surface	Inside	Surface	Inside	Surface	Inside
Constant rate period	A	Radical	Free water		Geometric optic		Low	
1st falling rate period Early part	B	Mild	Capillary condensed water	Free water	Mie / Rayleigh	Geometric optic	Moderate	Low
Late part	C	Moderate	Bound water	Free water	Rayleigh	Geometric optic	High	Low
2nd falling rate period	D	Radical		Bound water		Rayleigh		High

Topic IV

Effect of Cellular Structure on the Optical Properties of Wood

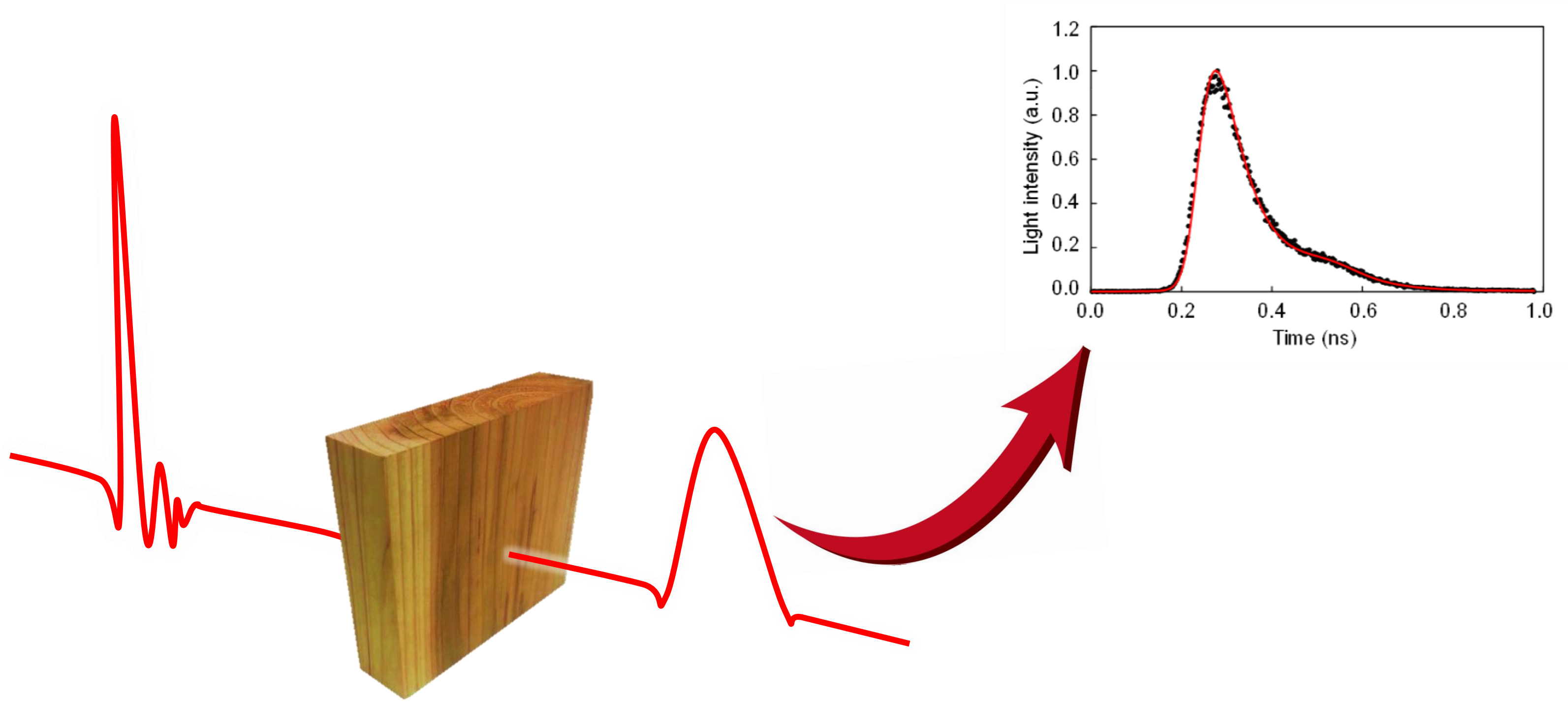

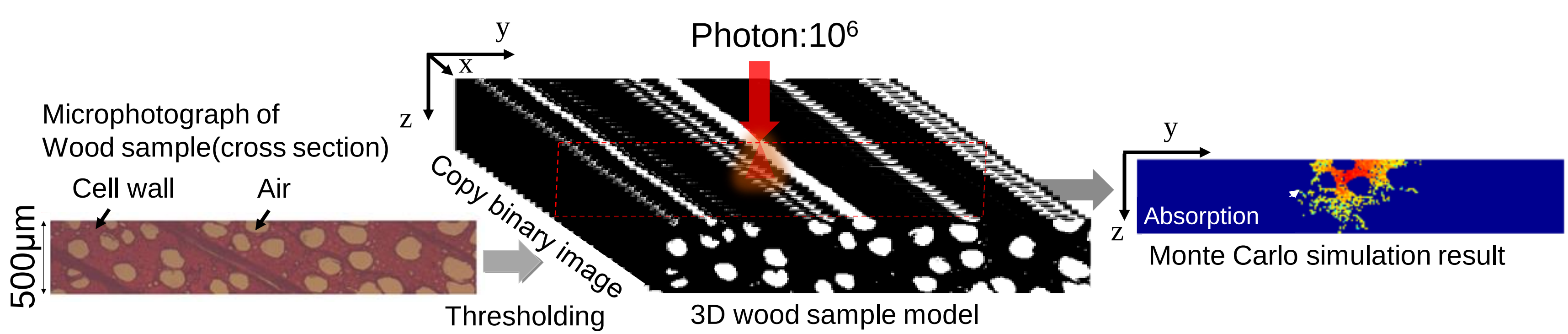

Microscopic images of (a) western red cedar (softwood), (b) beech (diffuse-porous vessel hardwood), and (c) castor aralia (ring-porous vessel hardwood). (d), (e) and (f) are the binary images of (a), (b) and (c), respectively.

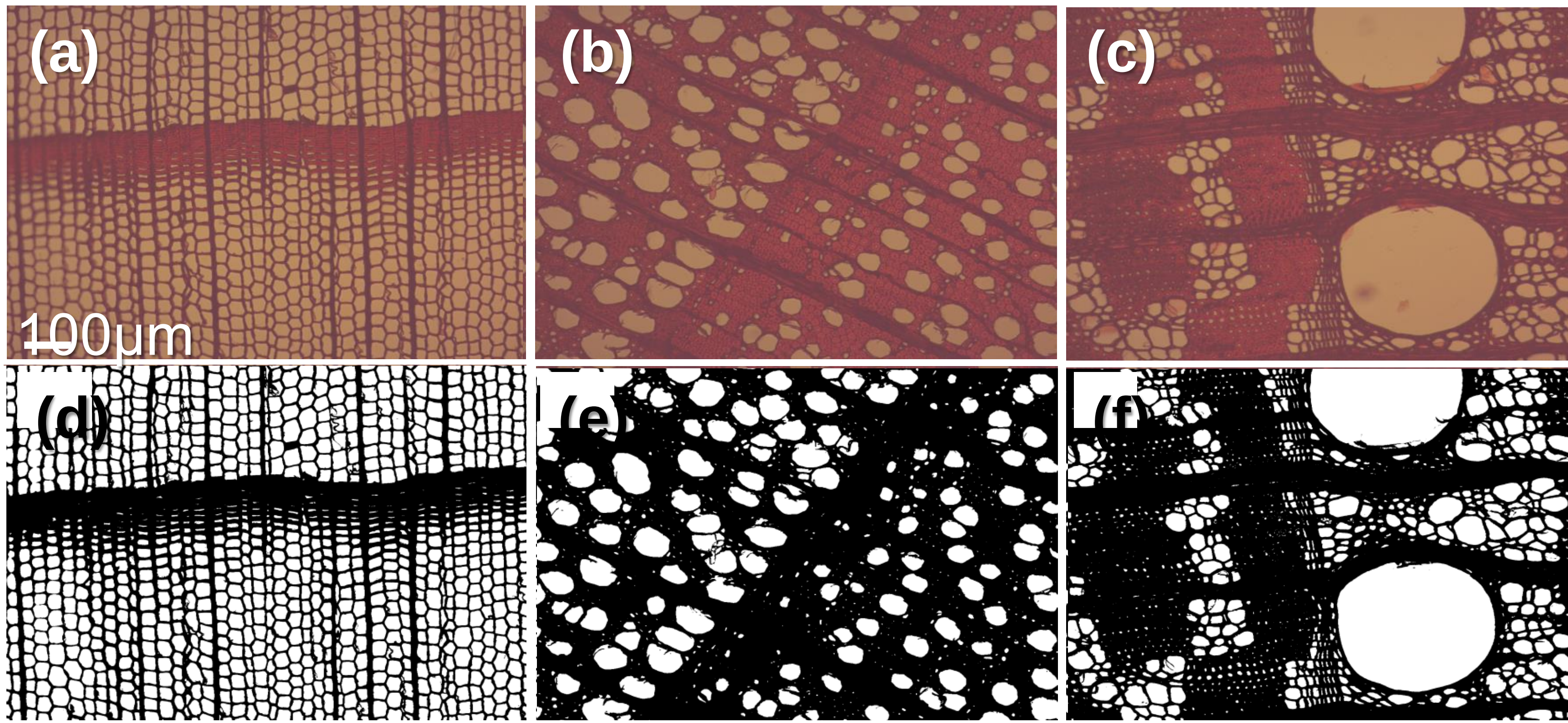

Which anatomical parameters affect light propagation in wood?

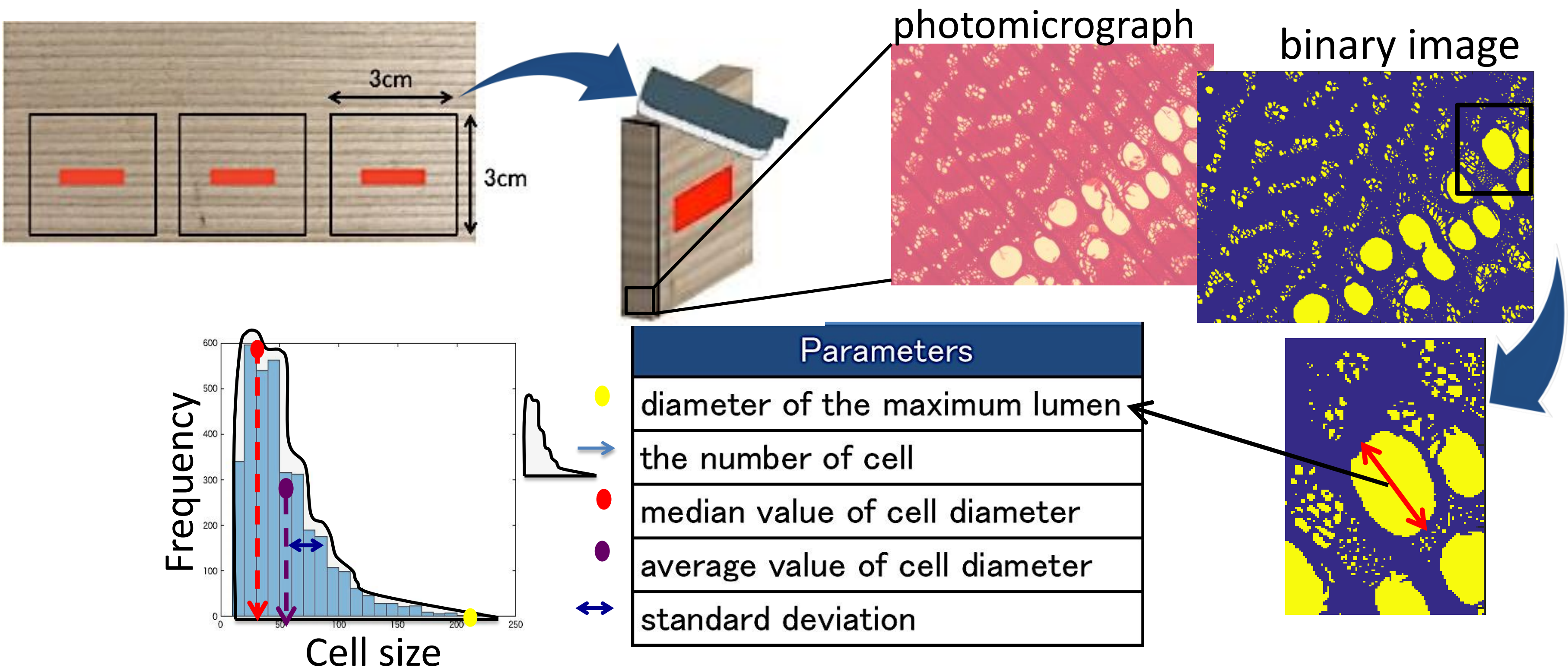

Relationship between Density and Measured Reduced Scattering Coefficient

Wood type	Species	Density (g/cm^3)	μ_s' (mm^{-1})
Softwood	*Agathis albaFoxw*	0.328±0.005	10.4±0.1
	Araucaria heterophylla	0.411±0.004	14.0±0.9
	Thuja plicata	0.360±0.010	11.1±0.7
	Chamaecyparis obtusa	0.446±0.010	12.5±0.2
	Cryptomeria japonica	0.335±0.004	9.9±1.8
Hardwood	*Triplochiton scleroxylon*	0.440±0.014	25.6±1.0
	Hevea brasiliensis	0.704±0.027	30.9±1.1
	Liriodendron tulipifera	0.508±0.008	14.2±0.9
	Cercidiphyllum Japonicum	0.400±0.015	8.9±0.5
	Paulownia tomentosa	0.287±0.002	12.9±0.7
	Kalopanax pictus	0.607±0.014	16.8±1.9
	Fraxinus mandshurica	0.638±0.021	21.4±0.4
	Fagus sylvatica	0.682±0.011	26.1±0.9

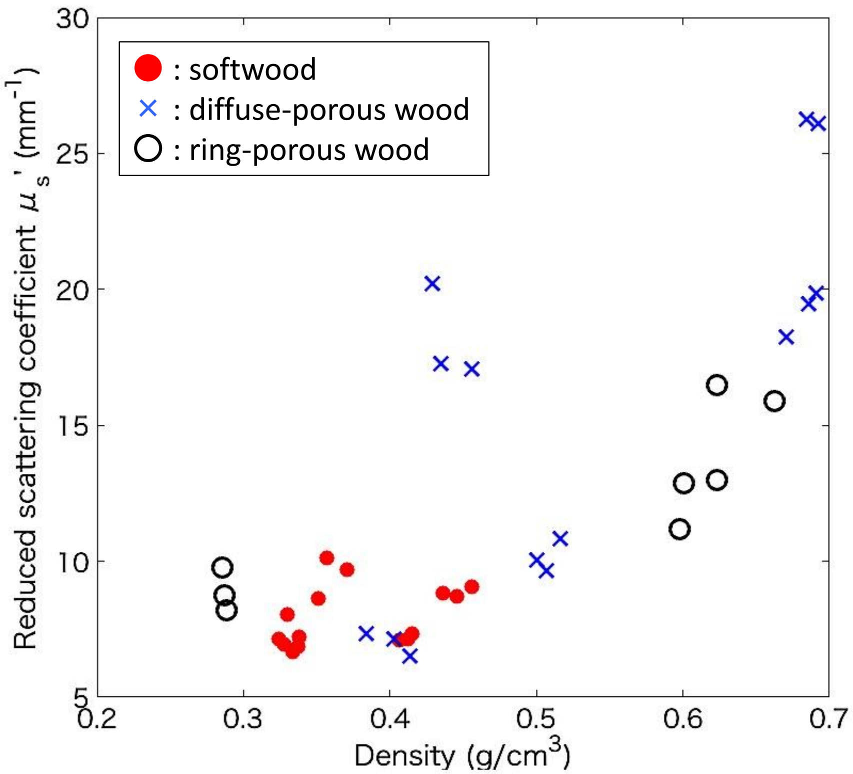

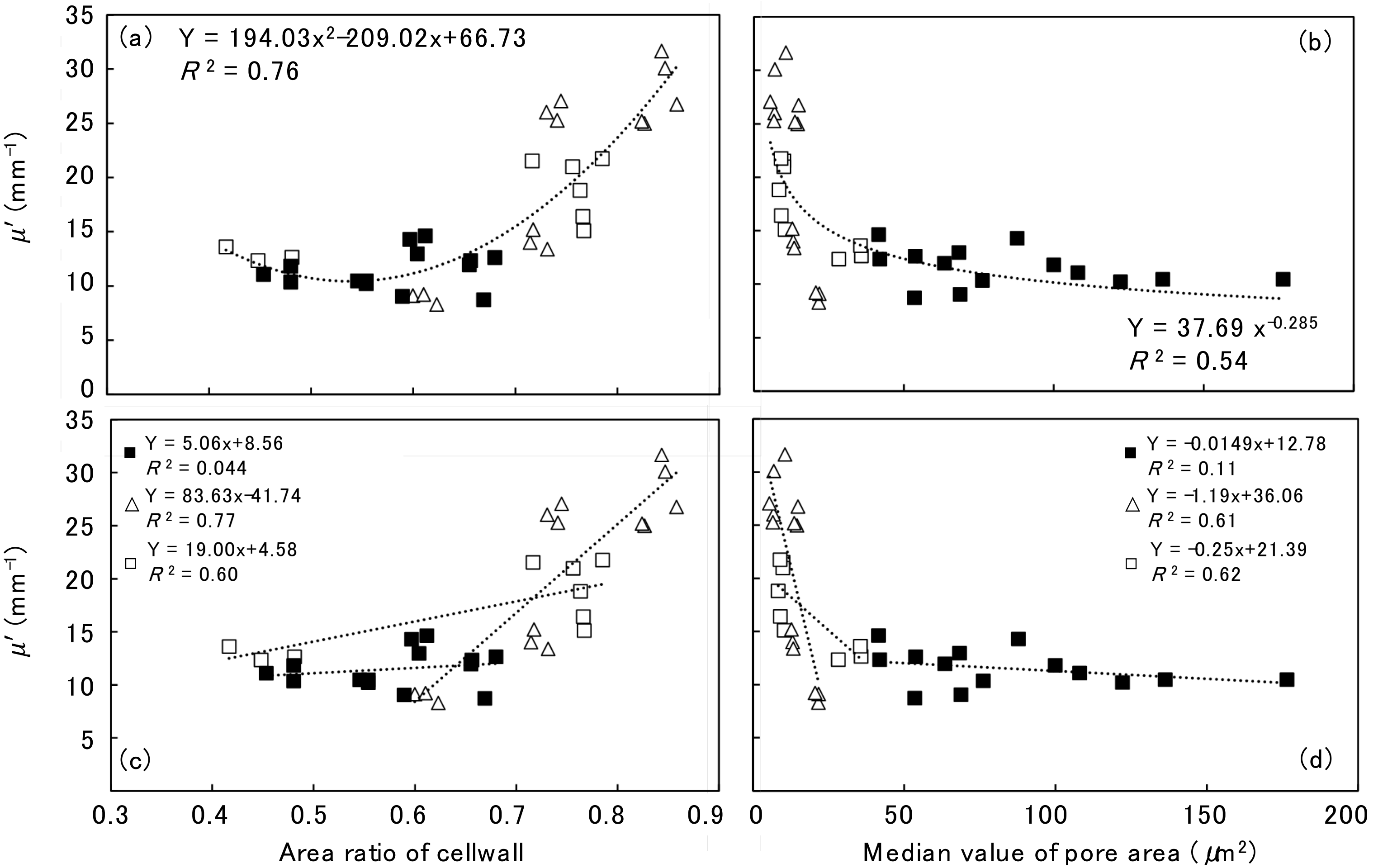

$$\mu_s' = a \times \rho_{airdry} + b \times r^2 + c \times r + d \times S^e + f.$$

r: Ratio of the cell wall

S: Median pore area

a, b, c, d, e, and f were determined by a nonlinear curve-fitting method.

Light Propagation in (a) Japanese cedar (b) Agathis (c) Empress tree (d) Yellow poplar and (e) Rubber wood simulated by the Monte Carlo method

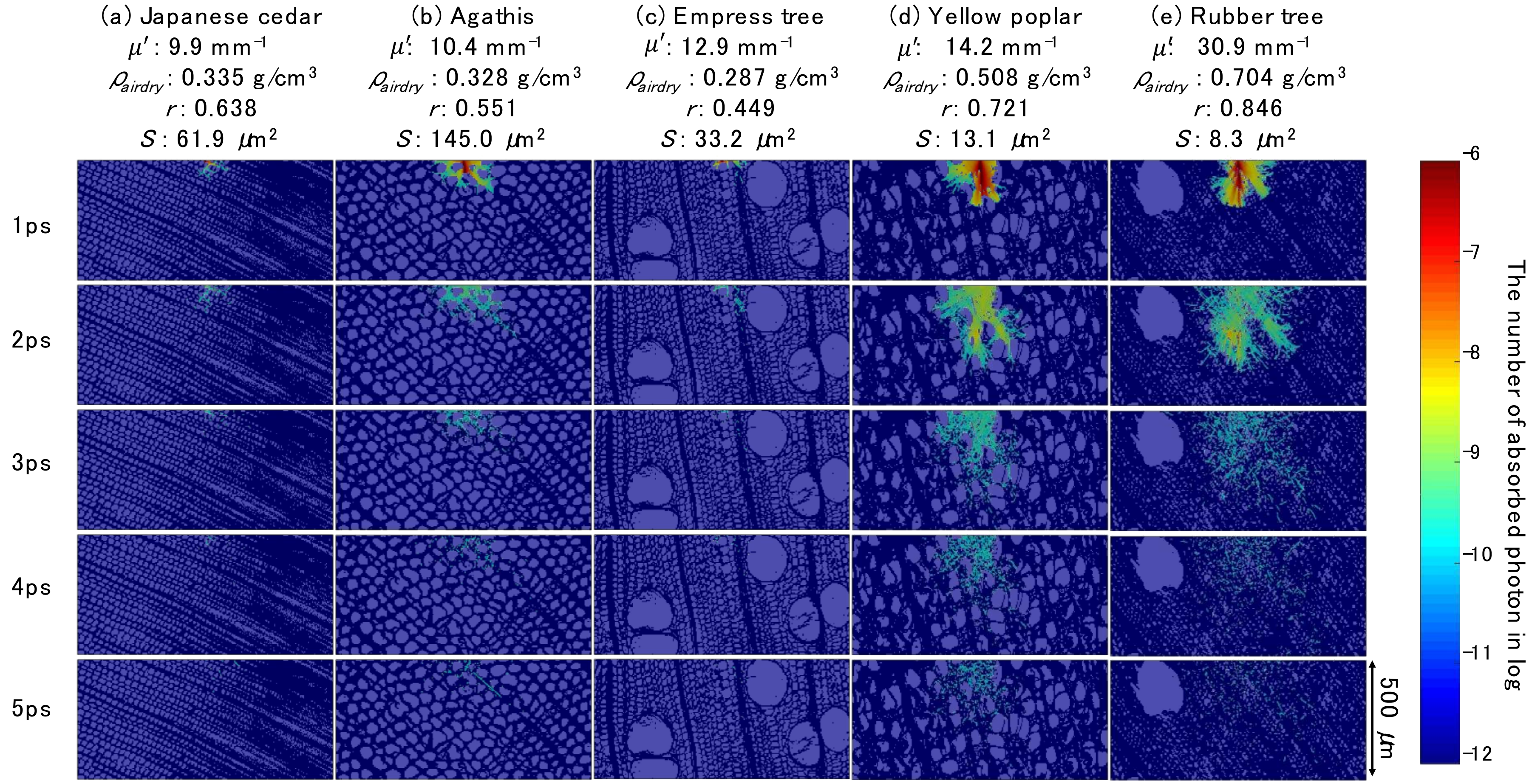

ρ_{airdry}: air dry density, r: Areal ratio of cell wall, S: Median value of pore area

Topic V

Three Fiber-based Diffuse Reflectance Spectroscopy (TFDRS) for Estimation of Total Solid Content in Natural Rubber Latex

Para rubber tree

Quality Control

Rubber product

$$\text{TSC}\ (\%) = \frac{\mathrm{M}_1}{\mathrm{M}_0} \times 100 \quad (\text{Eq. } 1)$$

M_0= Weight of latex sample, M_1=Weight of dried rubber sheet

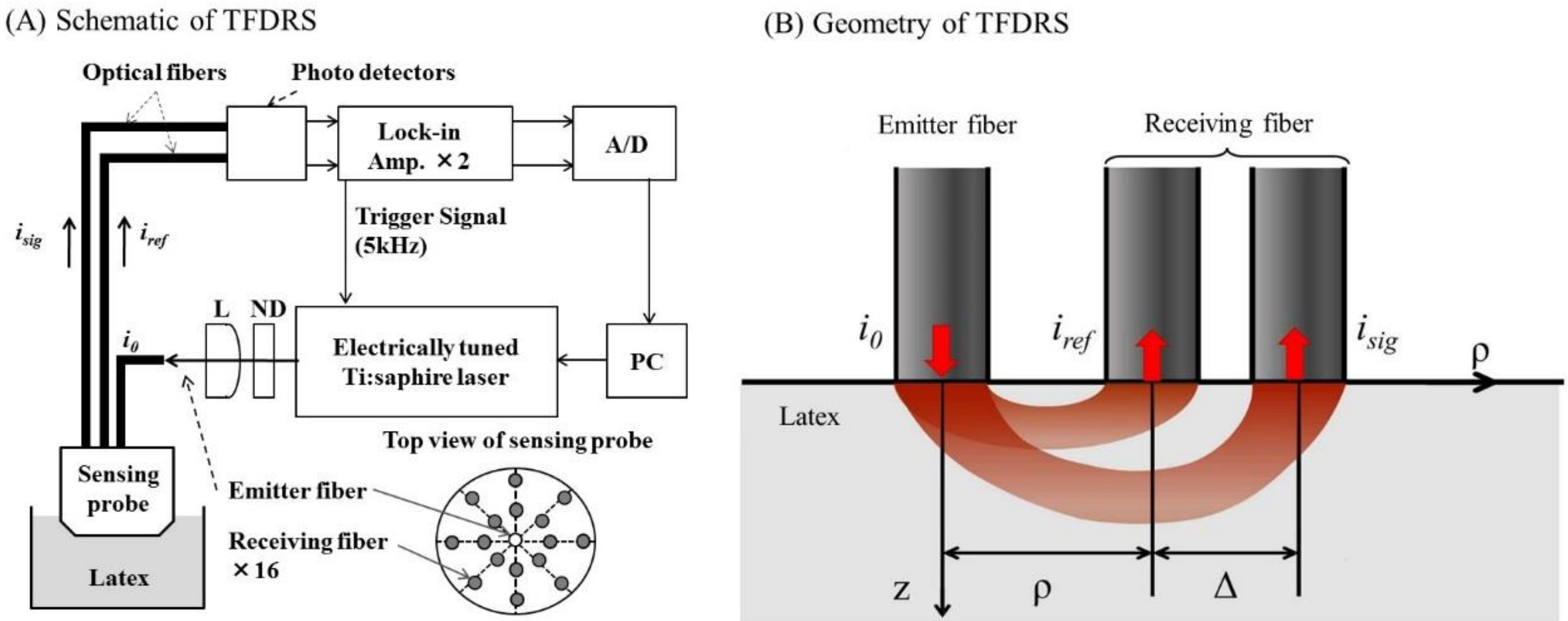

$$R = \frac{i_{sig}}{i_{ref}} \qquad \text{(Eq. 2)}$$

Relative absorbance ratio

$$\gamma(\lambda_1, \lambda_2, \lambda_3) = \frac{\log R(\lambda_2) - \log R(\lambda_1)}{\log R(\lambda_3) - \log R(\lambda_1)} \qquad \text{(Eq. 3)}$$

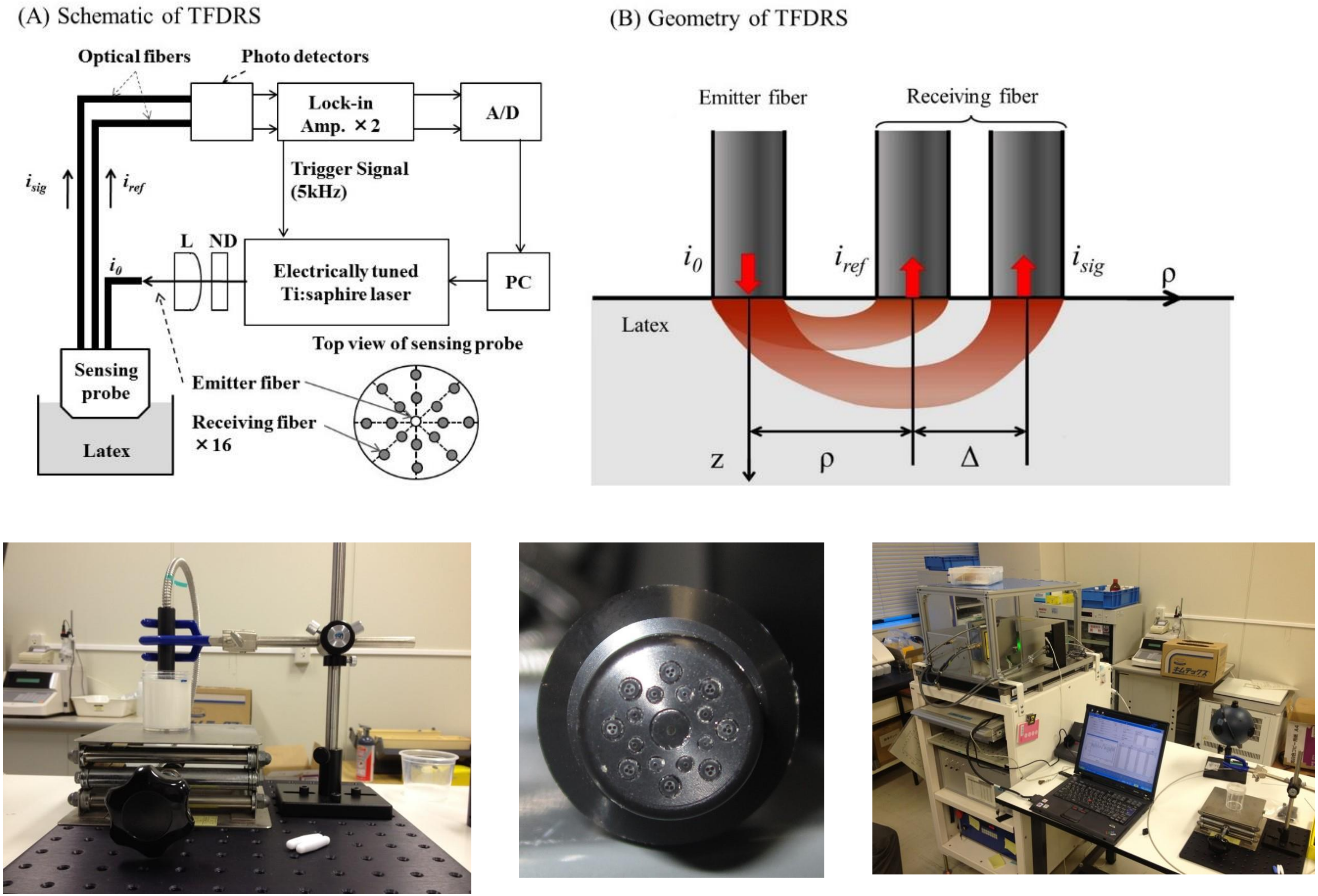
(A) Schematic of TFDRS
Optical fibers
Photo detectors
Lock-in Amp. ×2
A/D
Trigger Signal (5kHz)
i_{sig}
i_{ref}
i_0
L
ND
Electrically tuned Ti:saphire laser
PC
Top view of sensing probe
Sensing probe
Emitter fiber
Receiving fiber ×16
Latex
(B) Geometry of TFDRS
Emitter fiber
Receiving fiber
i_0
i_{ref}
i_{sig}
ρ
Latex
z
ρ
Δ

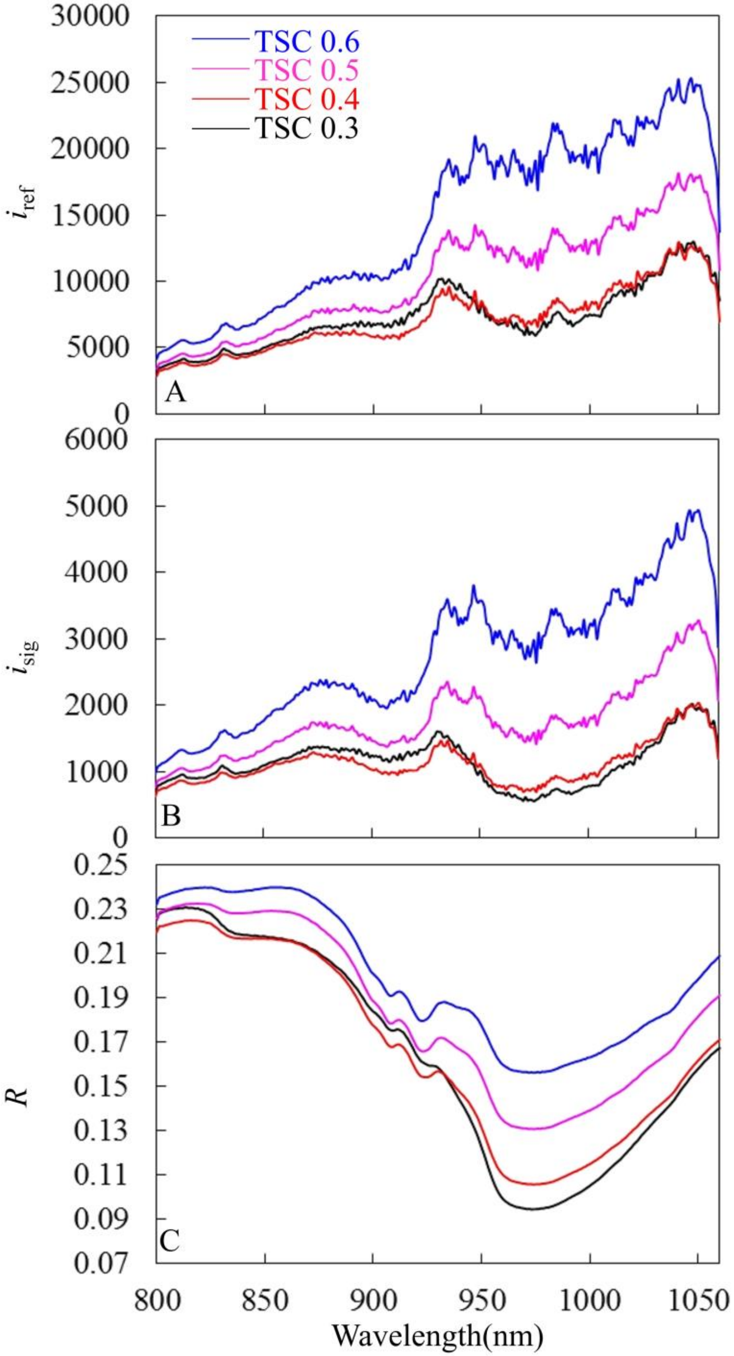

(A) Light intensity i_{ref} (2 mm)
(B) Light intensity i_{sig} (3 mm)
(C) Relative absorbance (R) of latex samples

Reflectance Ratio of Latex

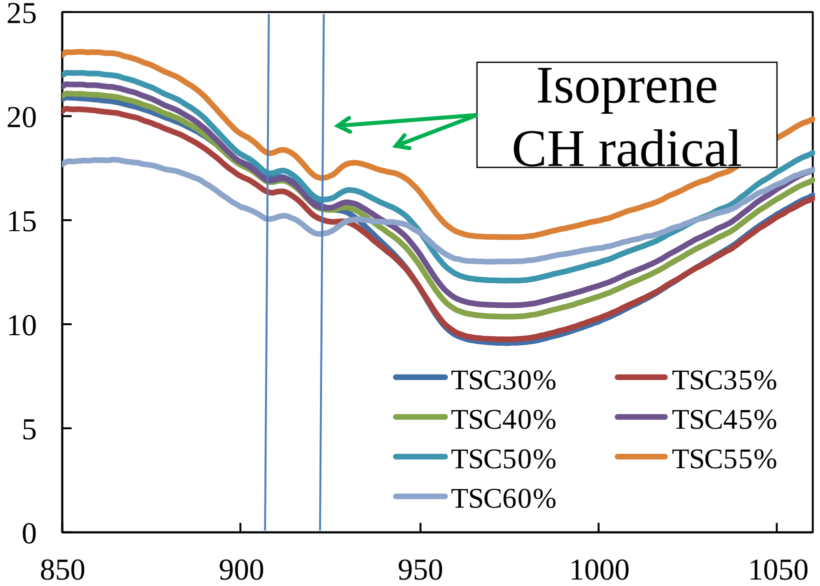

Relationship between Measured and Predicted TSC

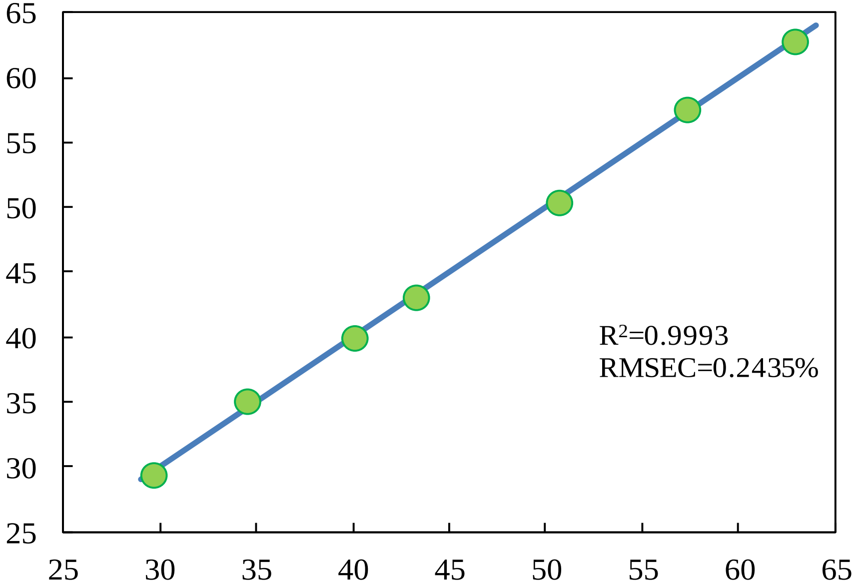

Calculated Scattering Coefficient and Absorption Coefficient

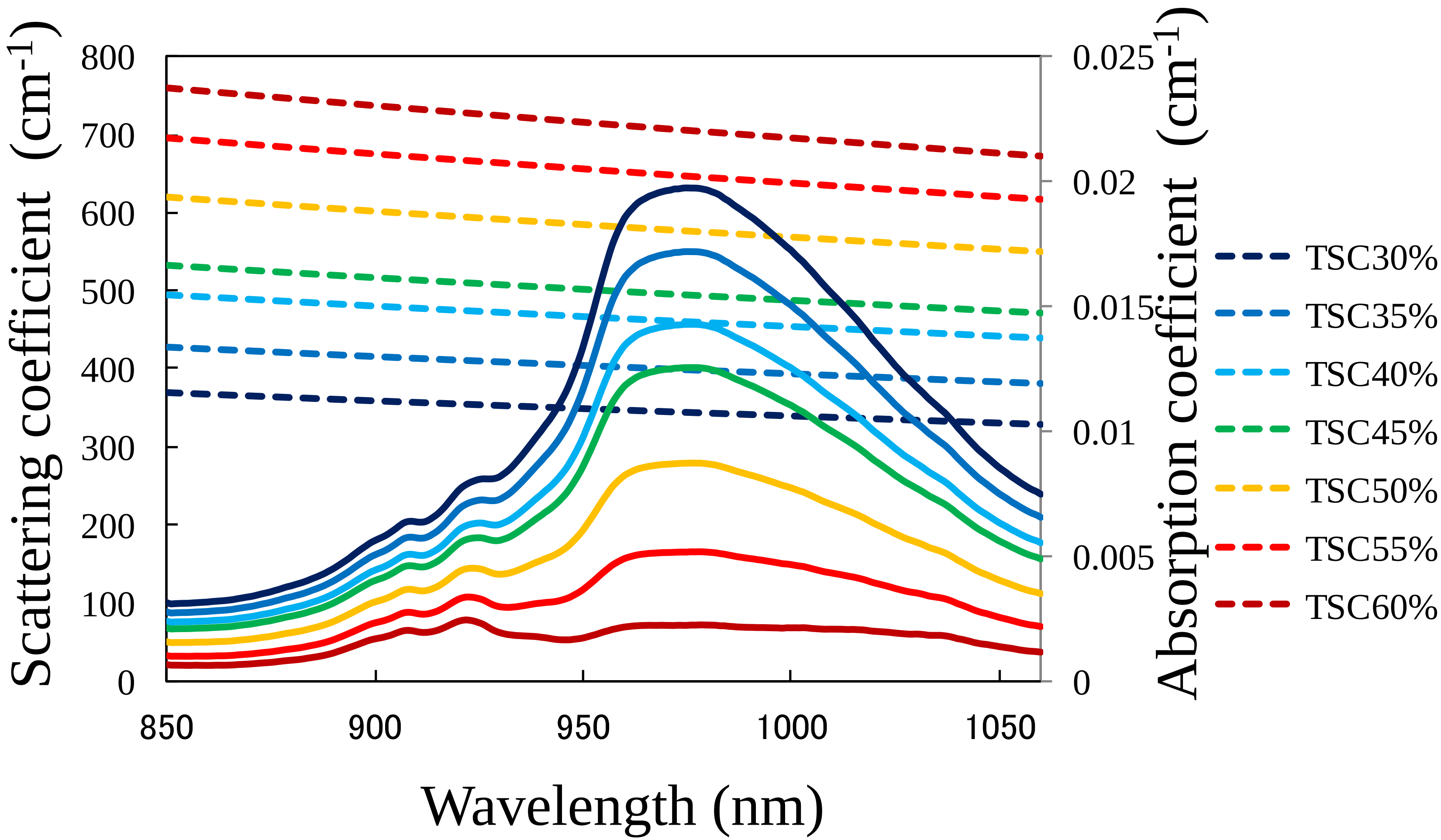

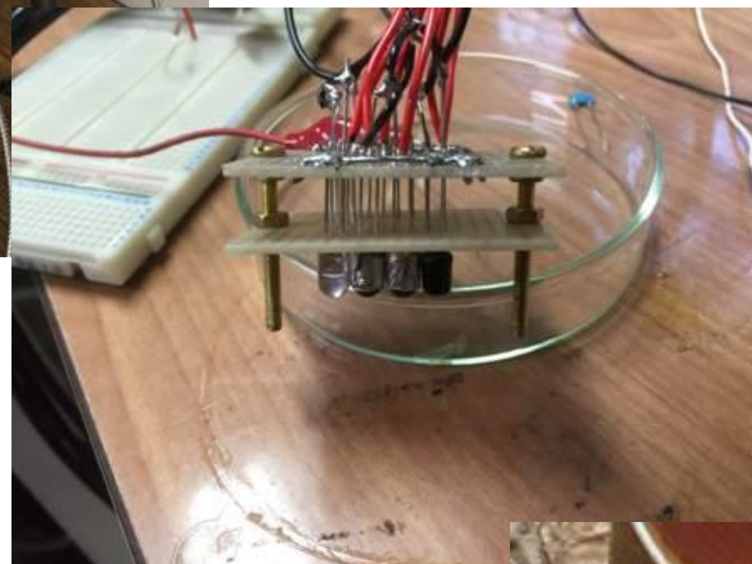

Topic VI

Optical Characteristics of Wood at various Densities, Grain Directions, and Thicknesses Investigated by NIR Spatially Resolved Spectroscopy (NIR-SRS)

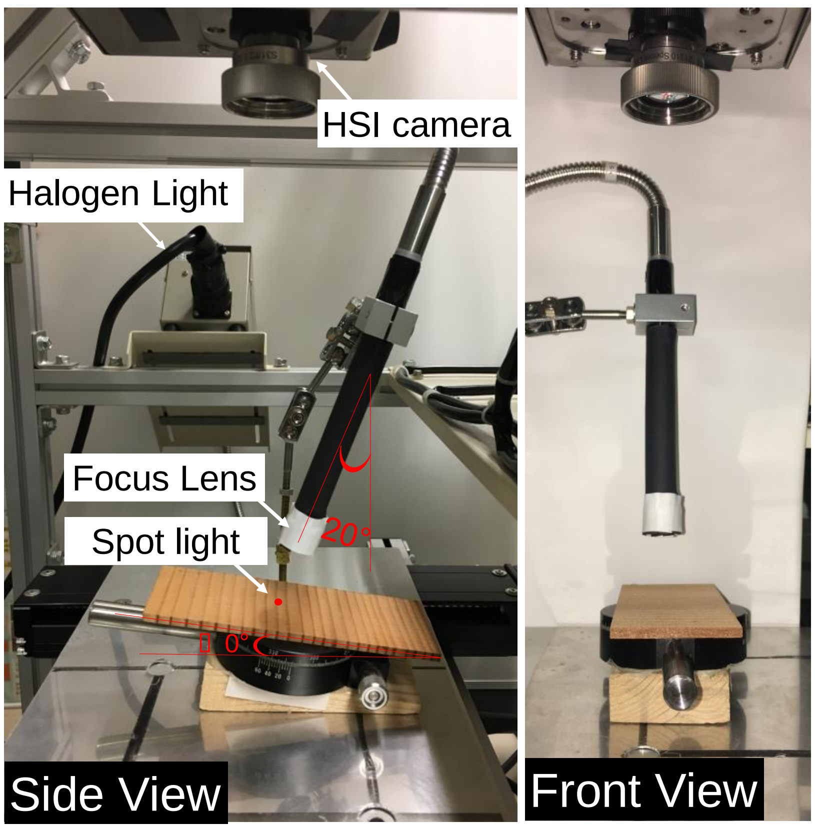

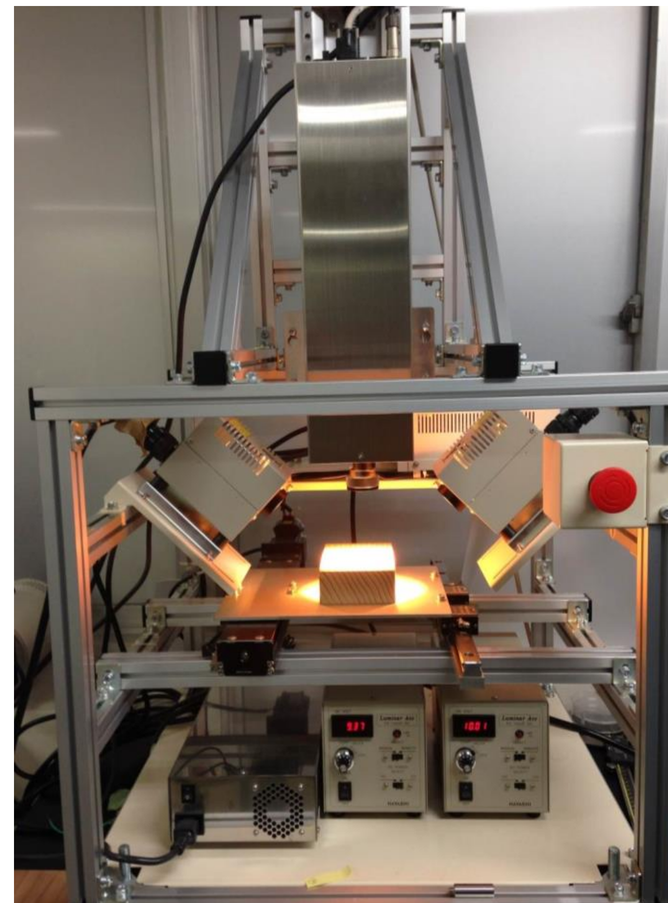

What we have done:

Mapping wood density and MFA at a very high spatial resolution

(NIR-HSI)

Can measure chemical bonds vibration non-destructively

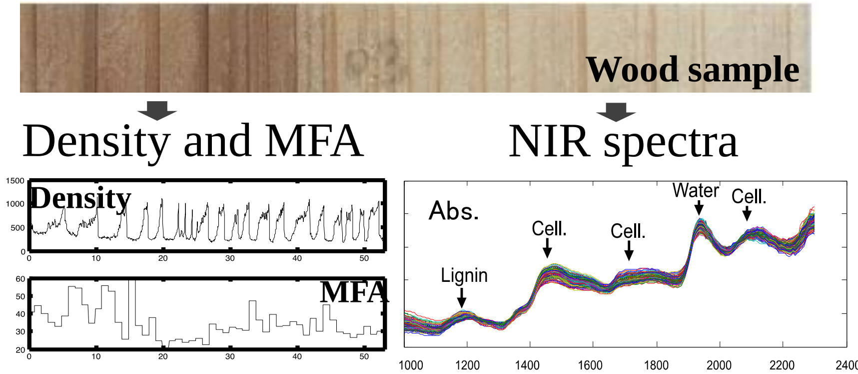

PLS regression analysis

Density mapping result

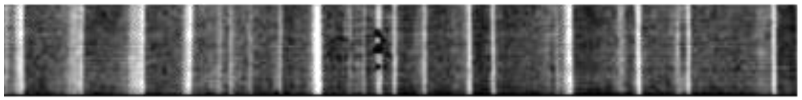

MFA mapping result

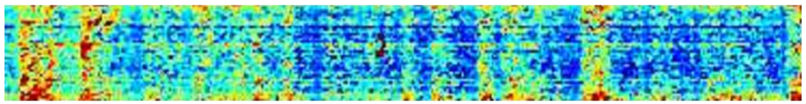

NIR spectra：

Only describe the aggregate effect of absorption and scattering

What are the issues:

A considerable amount of wavelength data is required, which is usually not transferable among instruments.

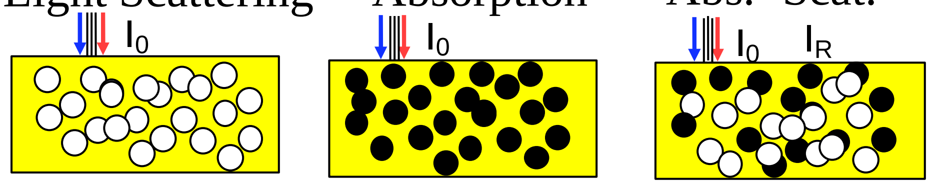

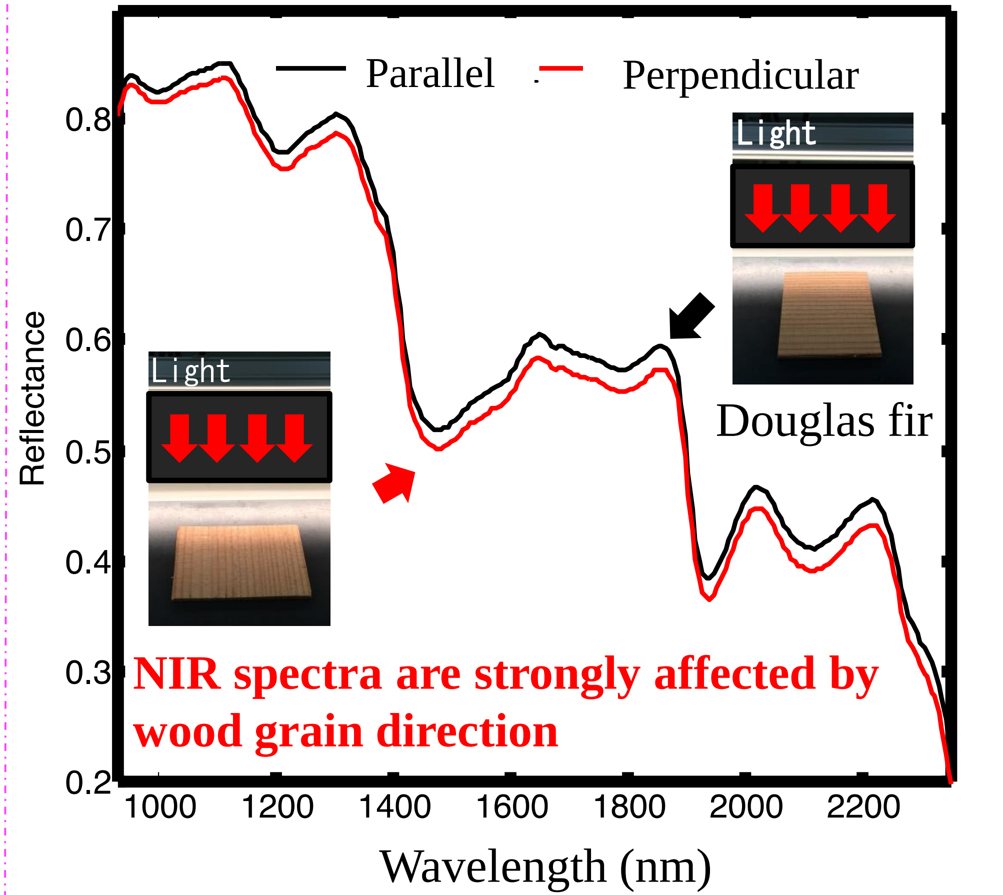

NIR-SRS (spatially resolved spectroscopy) was proposed

Simpler means for measuring the optical properties at a wide wavelength range

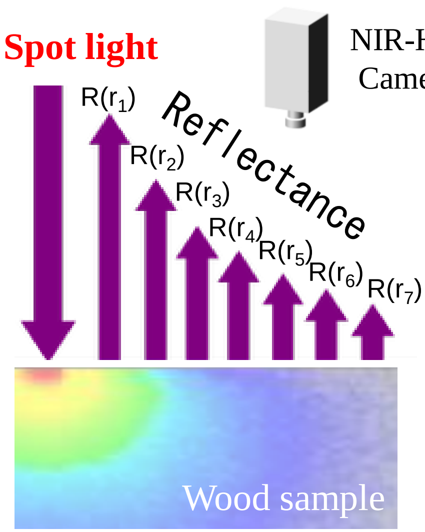

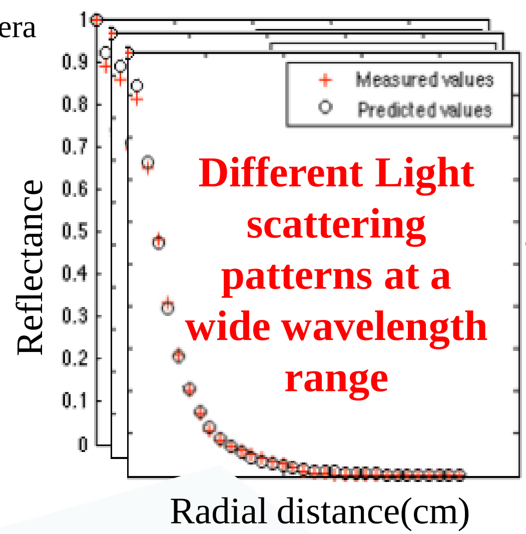

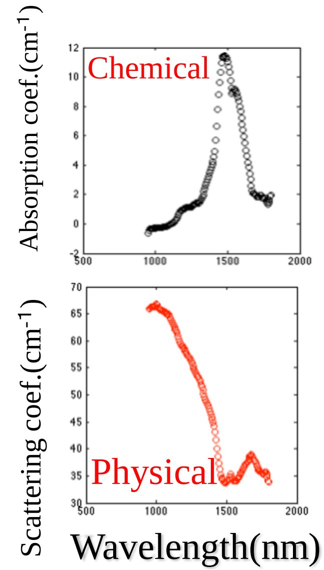

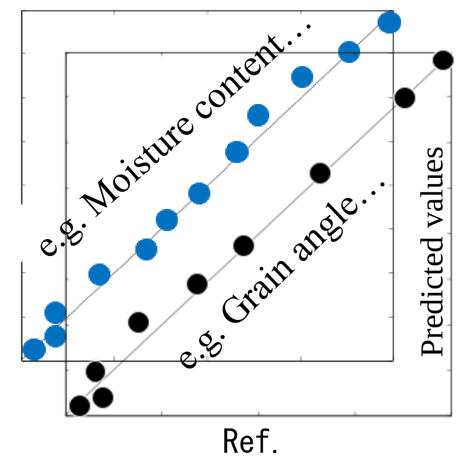

Building prediction models without multivariate analysis

$$R(r) = \frac{a'}{4\pi}\left[\frac{1}{\mu_t'}\left(\mu_{eff}+\frac{1}{r_1}\right)\frac{\exp(-\mu_{eff}r_1)}{r_1^2}+\left(\frac{1}{\mu_t'}+\frac{4A}{3\mu_t'}\right)\left(\mu_{eff}+\frac{1}{r_2}\right)\frac{\exp(-\mu_{eff}r_2)}{r_2^2}\right]$$

$$r_1 = \left[\left(\frac{1}{\mu_t'}\right)^2 + r^2\right]^{1/2}$$

$$r_2 = \left[\left(\frac{1}{\mu_t'}+\frac{4A}{3\mu_t'}\right)^2 + r^2\right]^{1/2}$$

$$a' = \frac{\mu_s'}{\mu_s'+\mu_a}$$

$$\mu_{eff} = [3\mu_a(\mu_a+\mu_s')]^{1/2}$$

μ_s': Scattering Coefficient
μ_a: Absorption Coefficient
Predict

R : Reflectance
r : Radial distance form spot light
Measure

Farrell, T.J., Patterson, M.S., Brain, W., 1992. Medphys 19, 879–888

Sample : Douglas fir [*Pseudotsuga menziesii* (Mirb.) Franco]

Size: 50 mm (Longitudinal) ×130 mm (Radial) ×1mm、3mm、5mm (Tangential)

Density measurement: X-ray densitometry (Scan interval 8.3 μm)

Beer's law Density

$$I = I_0 e^{-a_m D T}$$

thickness

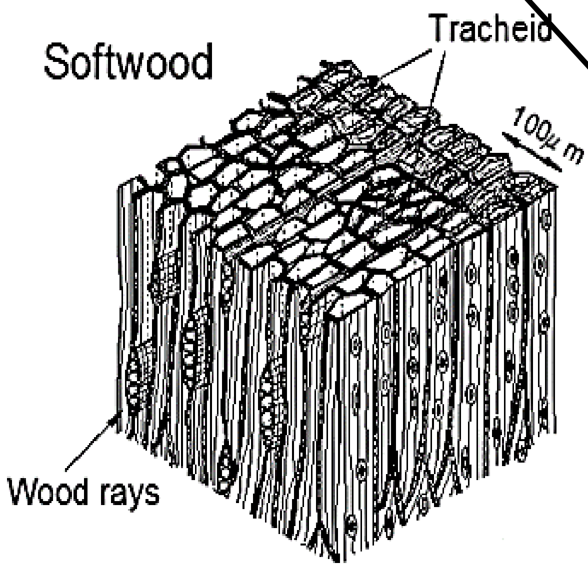

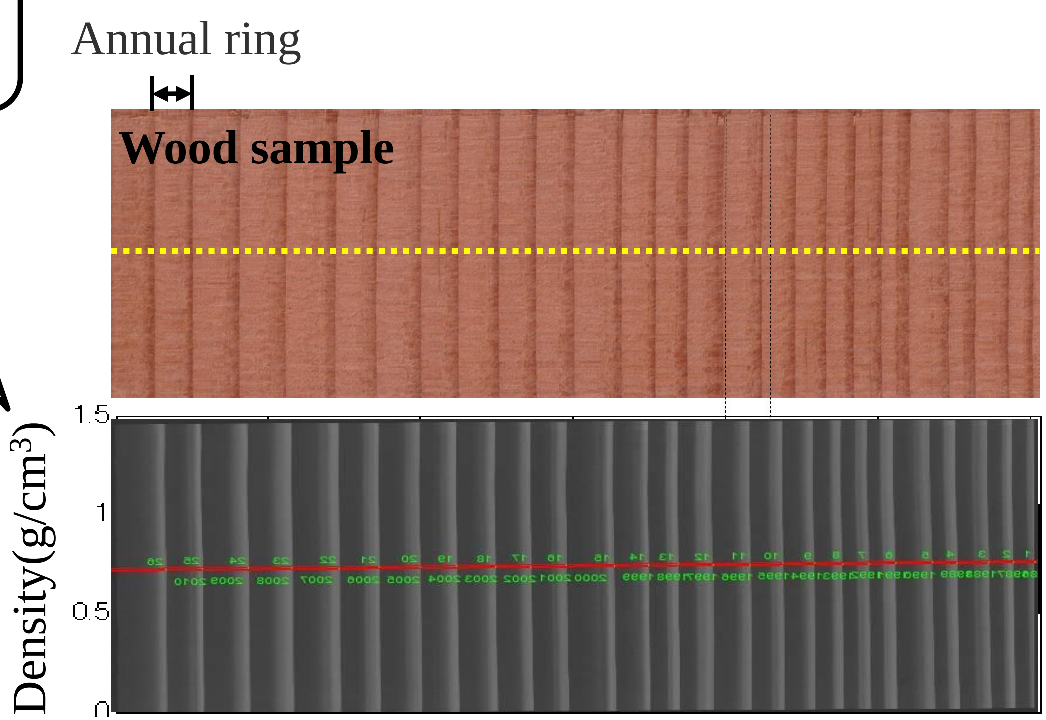

X-ray transmission image

Tracheid : over 90% (Volume ratio)

Spatial information (interval: 8.3μm)

Designed NIR-SRS (spatially resolved spectroscopy) system
How to predict wood grain angle?

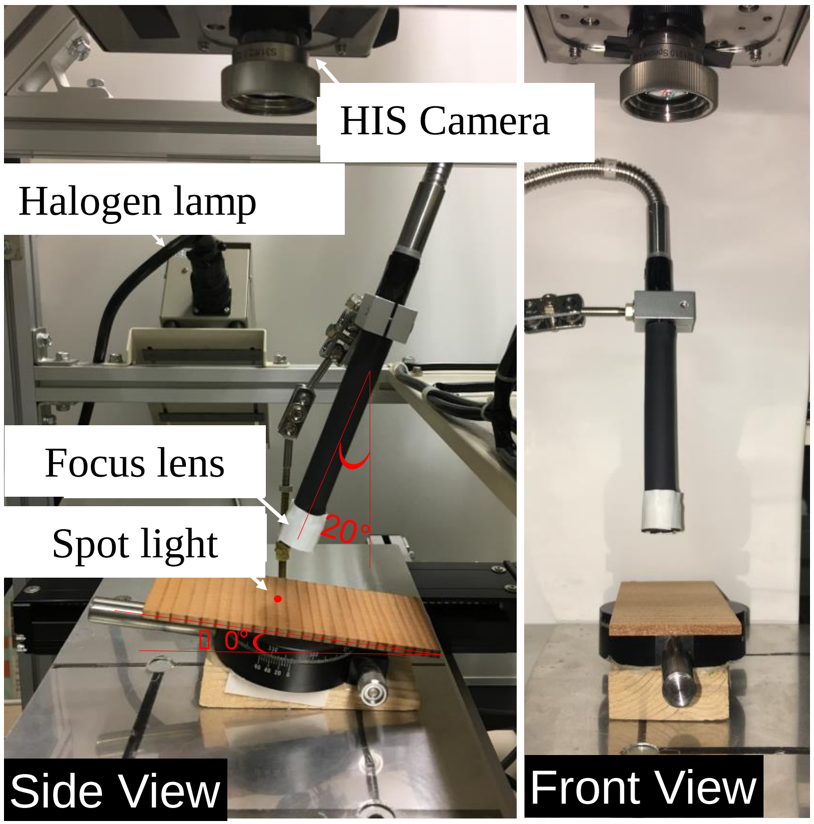

Designed NIR-HSI system

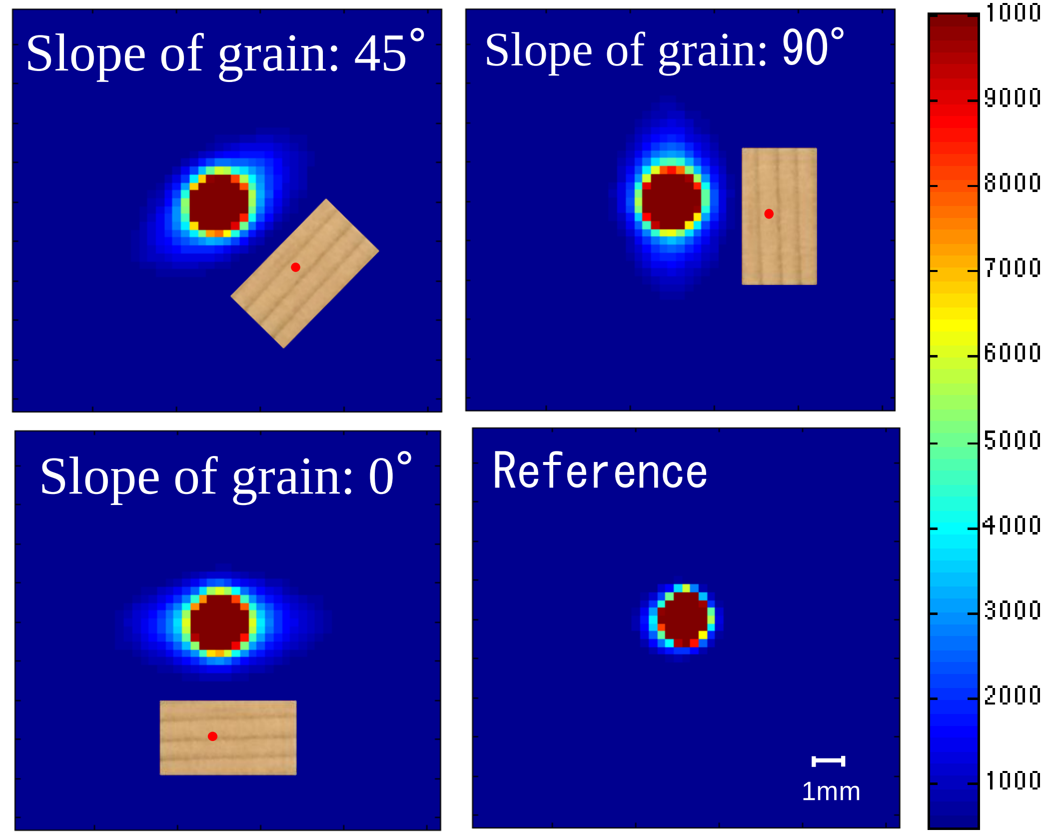

Spatial resolved image (Wavelength 1305nm)

The orientation of the scattering pattern depends on the grain direction

How to predict wood density?

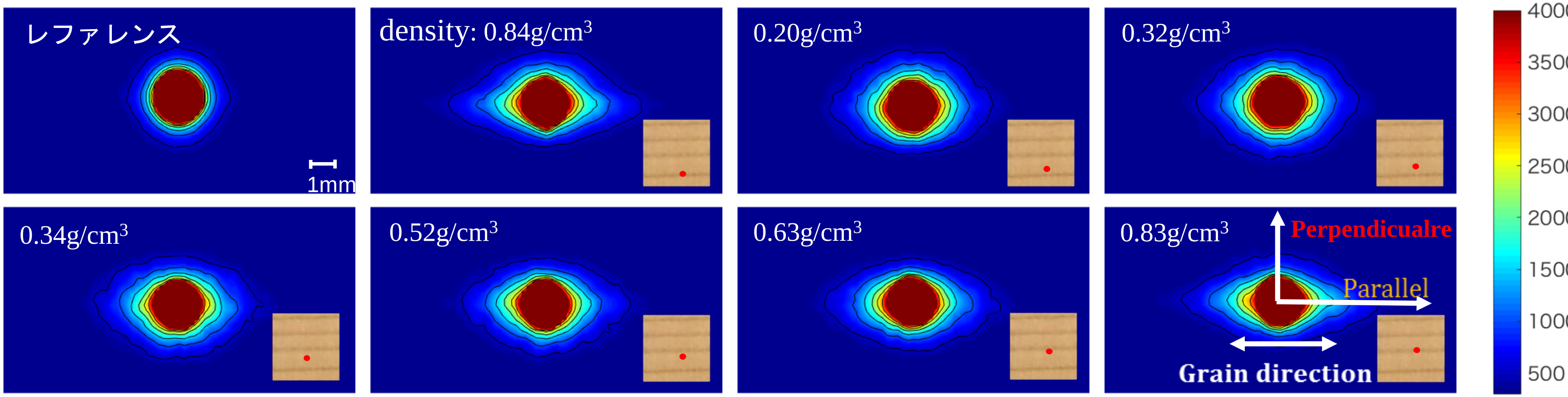

Spatially resolved images (wavelength1305nm)

Parallel to grain

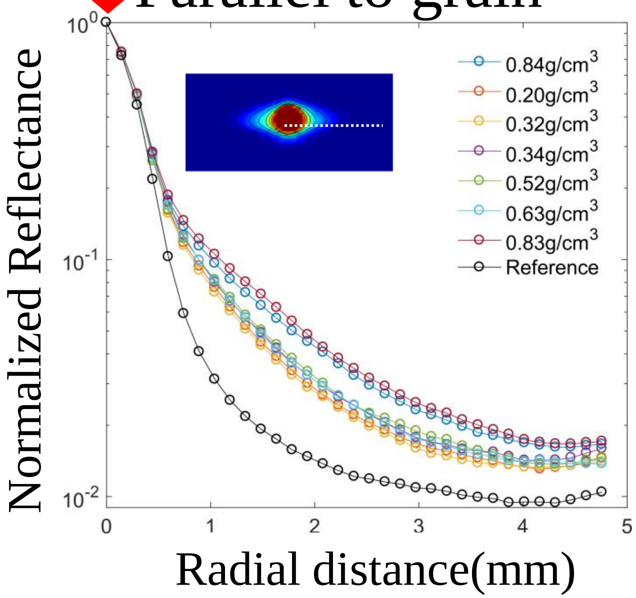

Perpendicular to grain

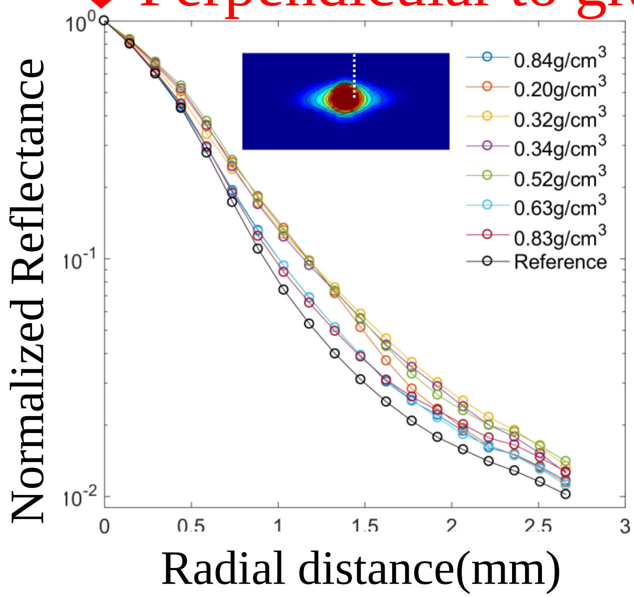

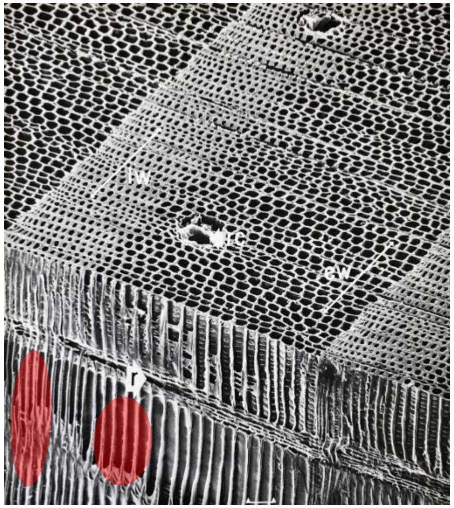

H.A. CORE, W.A. COTE, and A.C. DAY, Wood structure and identification, Syracuse wood science series, 6, 1979

NIR-SRS (spatially resolved spectroscopy) was proposed

Simpler means for measuring the optical properties at a wide wavelength range

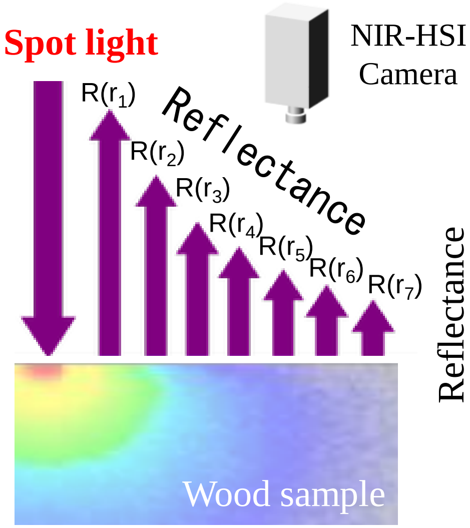

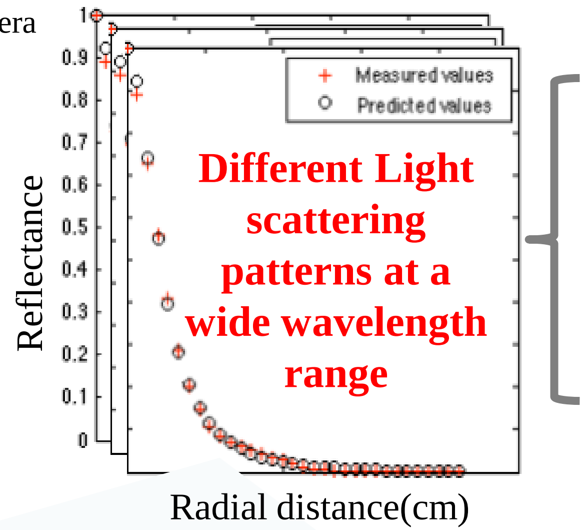

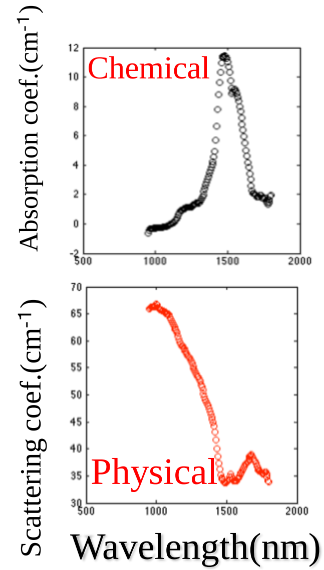

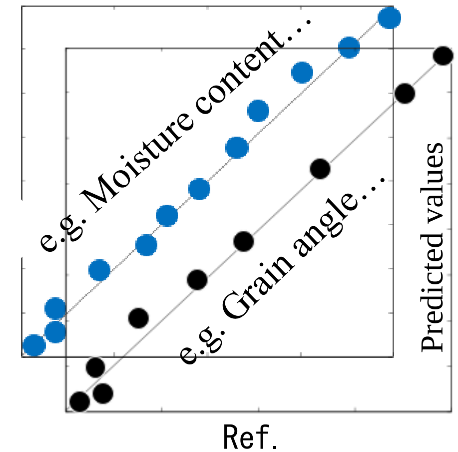

Building prediction models without multivariate analysis

$$\boxed{R(r)} = \frac{a'}{4\pi}\left[\frac{1}{\mu_t'}\left(\mu_{eff} + \frac{1}{r_1}\right)\frac{\exp(-\mu_{eff} r_1)}{r_1^2} + \left(\frac{1}{\mu_t'} + \frac{4A}{3\mu_t'}\right)\left(\mu_{eff} + \frac{1}{r_2}\right)\frac{\exp(-\mu_{eff} r_2)}{r_2^2}\right]$$

$$r_1 = \left[\left(\frac{1}{\mu_t'}\right)^2 + r^2\right]^{1/2}$$

$$r_2 = \left[\left(\frac{1}{\mu_t'} + \frac{4A}{3\mu_t'}\right)^2 + r^2\right]^{1/2}$$

$$a' = \frac{\mu_s'}{\mu_s' + \mu_a}$$

$$\mu_{eff} = \left[3\mu_a\left(\mu_a + \mu_s'\right)\right]^{1/2}$$

μ_s': Scattering Coefficient

μ_a: Absorption Coefficient

R : Reflectance

r : Radial distance form spot light

Correlation between Optical Properties and Wood Density (Thickness: 1 mm)

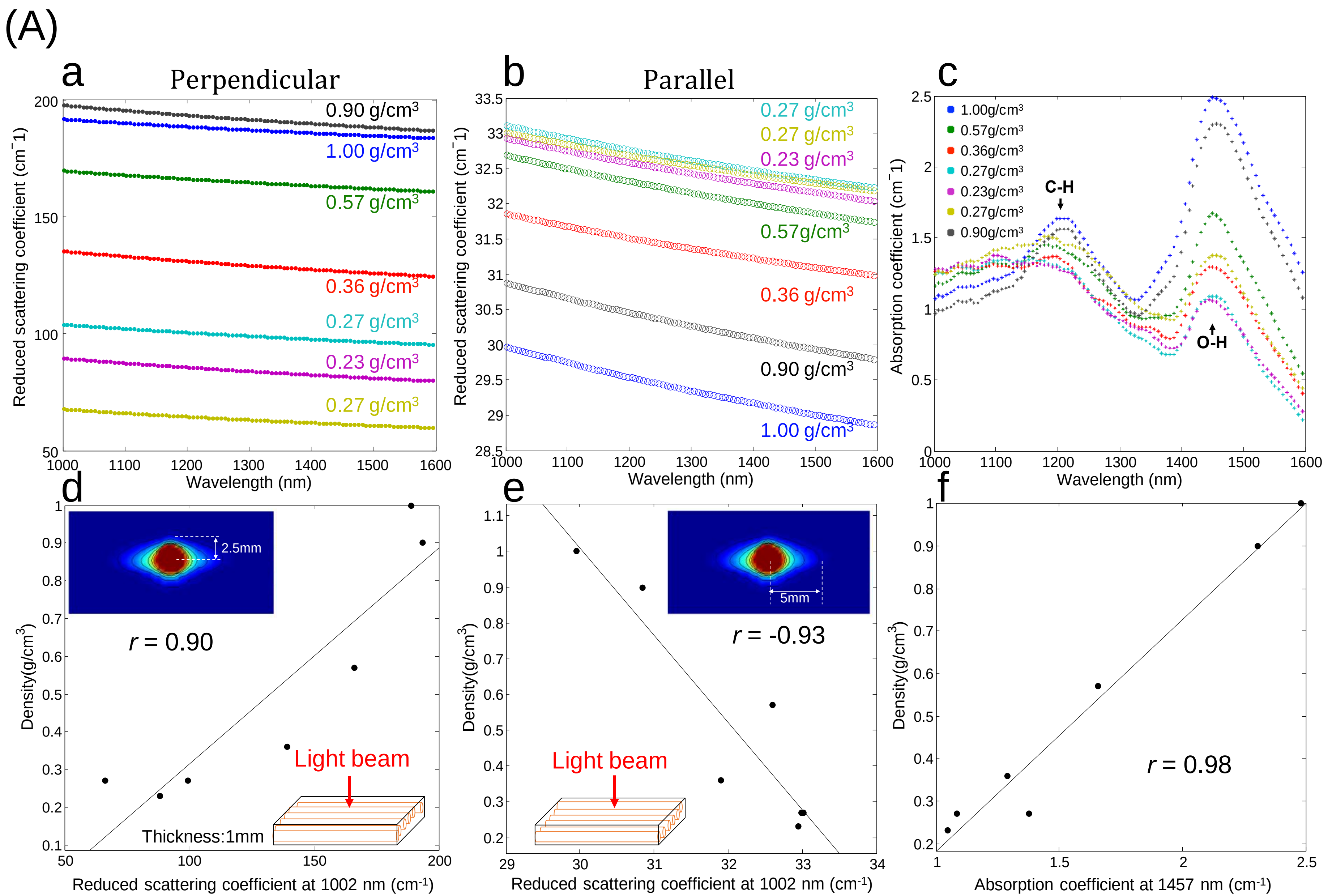

Correlation between Optical Properties and Wood Density (Thickness: 3 mm)

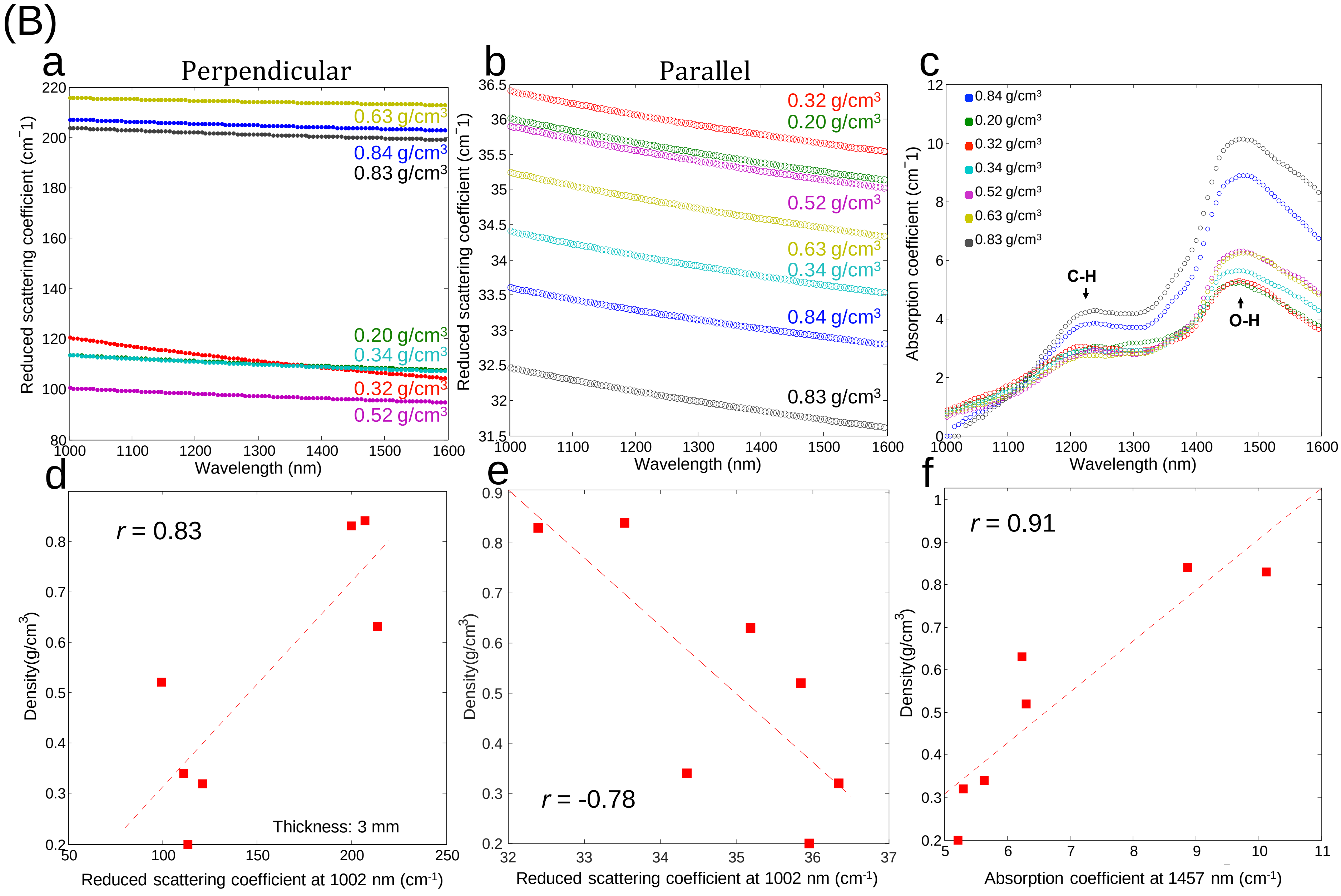

Correlation between Optical Properties and Wood Density (Thickness: 5 mm)

(C)

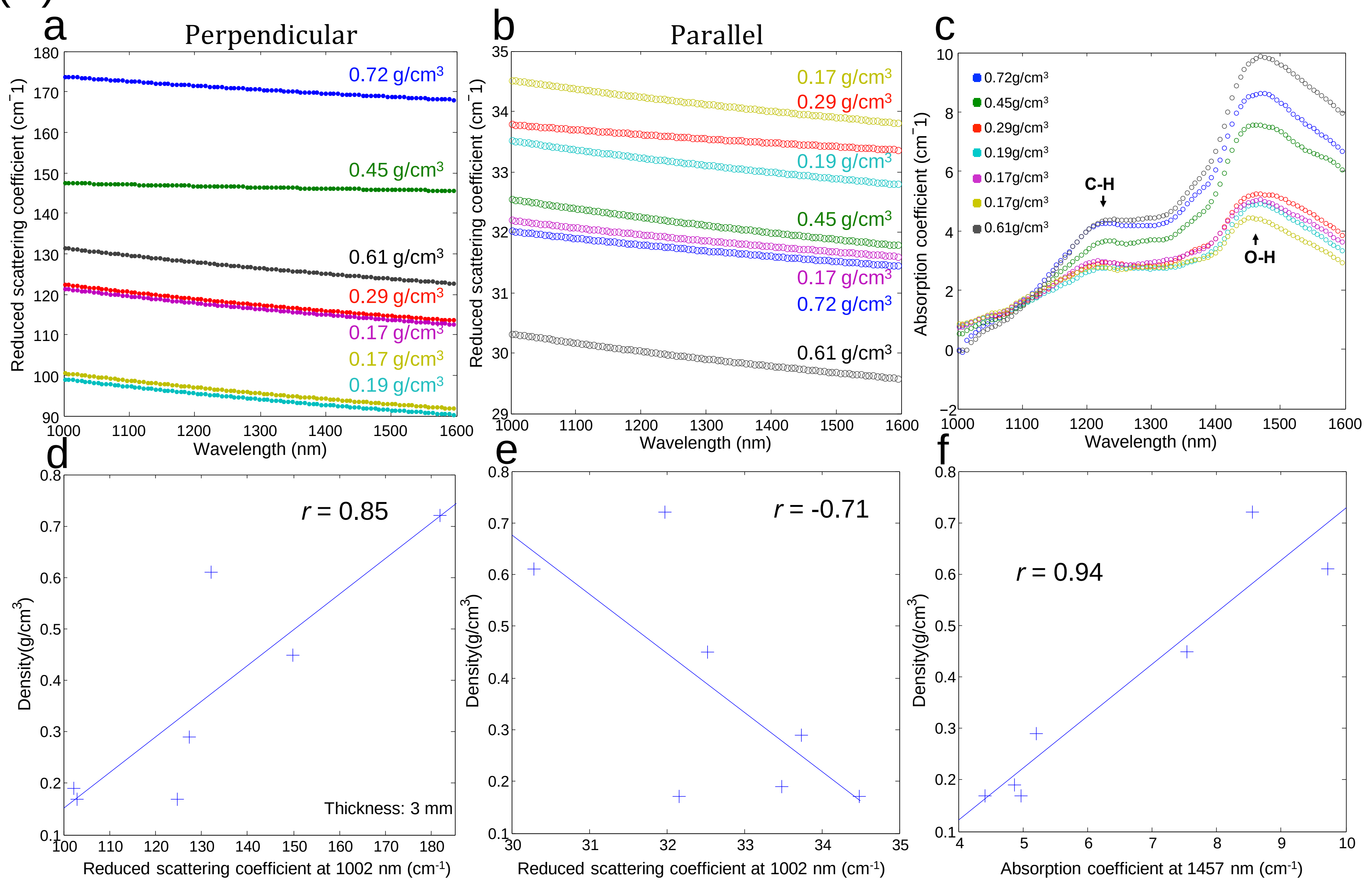

Satisfied wood density prediction accuracy was achieved by using two key wavelengths optical properties without complex chemometrics such as, PLS, PCR…

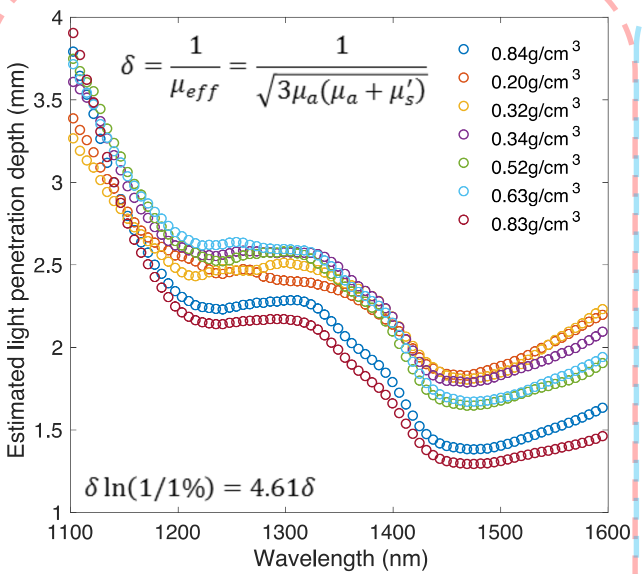

Light penetration depths

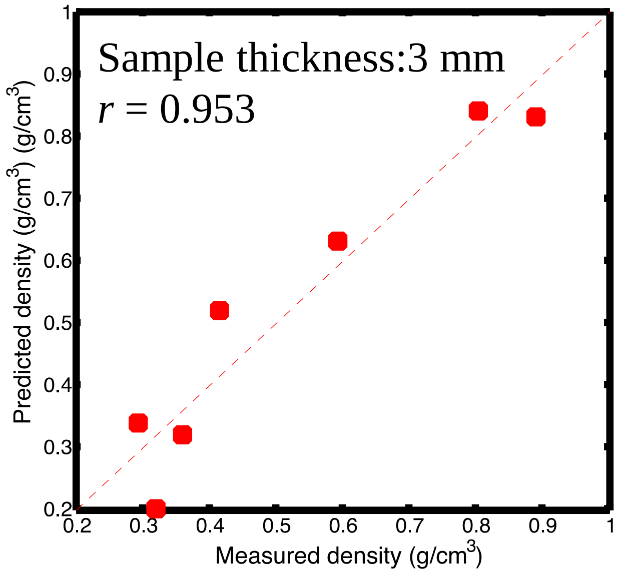

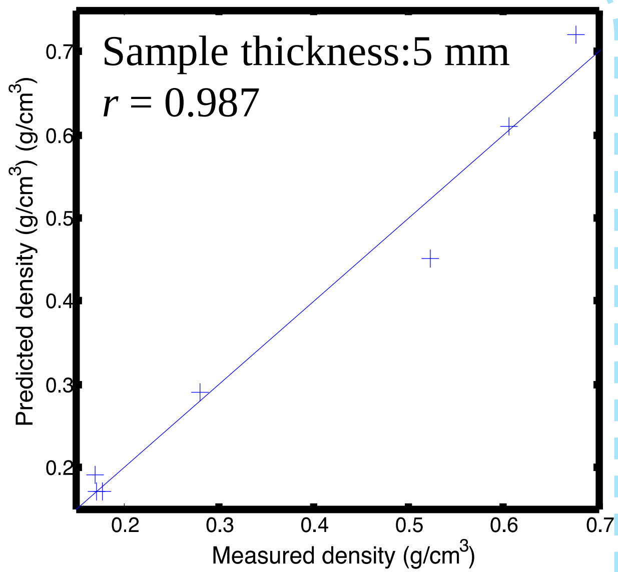

Scatter plot between measured wood densities and predicted values

$$D_{3mm} = -2.137 + 0.115 \times \mu_a - 0.046 \times \mu_s'(par.) + 0.002 \times \mu_s'(per.)$$

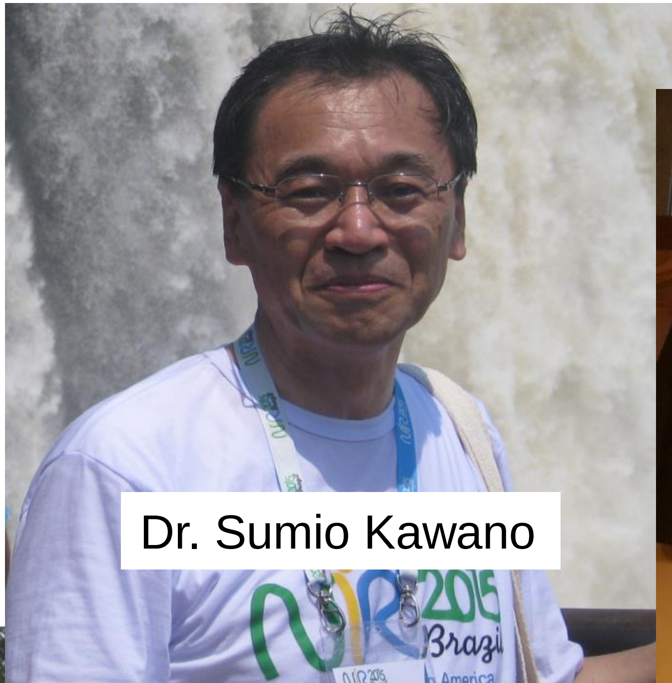
Dr. Sumio Kawano


Dr. Te Ma
Dr. Tetsuya Inagaki